Journal of Nuclear Medicine, published on December 11, 2020 as doi:10.2967/jnumed.120.257402

^{11}C dosimetry scans should be abandoned

Paolo Zanotti-Fregonara[1], Adriaan A Lammertsma[2], Robert B Innis[1]

1 Molecular Imaging Branch, National Institute of Mental Health, Bethesda, Maryland
2 Department of Radiology and Nuclear Medicine, Amsterdam UMC, location VUmc, Amsterdam, Netherlands

Corresponding author:

Paolo Zanotti Fregonara

Molecular Imaging Branch

National Institute of Mental Health

10 Center Drive, MSC-1026

Bldg. 10, Rm. B1D43

Bethesda, MD 20892-1026

Tel: 301-451-8898

Email: zanottifregonp@nih.gov

The views expressed in this commentary do not necessarily represent the views of the National Institutes of Health, the Department of Health and Human Services, or the United States Government.

Before a new tracer can be used in clinical research, it is customary to perform dosimetry scans in animals and humans to assess whether the radiation exposure is acceptable. The main parameter to assess the radiation exposure is the effective dose (ED), which is expressed in Sieverts and defined as the tissue-weighted sum of the equivalent doses in the different organs. According to the U.S. Food and Drug Administration, new radiotracers require an Investigational New Drug Application (IND). Although there are no formal dose limitations for INDs, most institutions limit the yearly ED from research scans to 50 mSv. European countries apply a limit of 10 mSv for minor-to-intermediate risk levels, based on the Medical Exposures Directive (97/43/Euratom) established by the European Commission. Sometimes, the dose to individual organs is needed as well, especially for tracers administered under the conditions specified in the Radioactive Drug Research Committee (RDRC) regulations.

New PET tracers are commonly labeled with either ^{11}C or ^{18}F. However, these two isotopes are different from a dosimetric standpoint, because the average ED of ^{11}C-tracers (5.2 ± 1.7 μSv/MBq; n=77) (Suppl. Table 1) is about one fourth the average ED from ^{18}F-tracers (20.5 ± 7.6 μSv/MBq; n=144) (Suppl. Table 2). In addition, ^{11}C doses have a smaller variability compared to ^{18}F doses: the dose range is 3.2 to 14.1 μSv/MBq for ^{11}C (a four-fold difference) and 3.7 to 50 μSv/MBq for ^{18}F (a ratio of 13.5).

With this letter, we argue that performing ^{11}C dosimetry scans is antithetical to two widely accepted principles that govern medical ethics committees, namely (1) to reduce animal experimentation and (2) to avoid unnecessary radiation exposure to the general public.
Instead, ^{11}C dosimetry scans for new tracers should be abandoned in both animals and humans and replaced by a standard average dose of 5 μSv/MBq. This would not compromise the safety of healthy volunteers and patients and would not significantly reduce the accuracy of dose estimation because (1) dose calculations in animals, even primates, have little predictive value for humans and (2) the results obtained from human dosimetry, both in terms of ED and organ dose, are mostly dependent on how the dose is calculated.

As Figure 1 clearly shows, ^{11}C dosimetry estimations are remarkably consistent, with only one outlying value: the dose of 14.1 μSv/MBq for the serotonin 1A receptors tracer ^{11}C-WAY-100635 (*1*), which stands at about seven standard deviations from the average of the other ^{11}C tracers. Arguably, extreme dose values may be explained by methodological issues, rather than biodistribution. The dosimetry of ^{11}C-WAY-100635 in rats was estimated at 4.1 μSv/MBq (unpublished data from MRC Cyclotron Unit, Hammersmith Hospital, London). In addition, tracers for the same target, and labeled with the same isotope, should not be radically different from a biological and biophysical point of view: the ED of ^{11}C-CUMI-101, also a tracer for Serotonin 1A receptors, is only 5.3 μSv/MBq (*2*). In any case, even if the dose of 14.1 μSv/MBq for ^{11}C-WAY-100635 was correct, it would still be about one standard deviation below the average dose for ^{18}F tracers. Notably, the ^{18}F group also has one major outlier: the dose from ^{18}F-tetrafluoroborate was estimated at the very high value of 50 μSv/MBq in healthy volunteers (average between the male dose at 36 μSv/MBq and the female dose at 64 μSv/MBq) in one study (*3*), but at 32.6 μSv/MBq by another study (*4*), despite the dose being calculated in thyroid cancer patients, and no significant differences between males and females were reported.

Even without considering extreme outliers, variations around the mean values are largely due to how the dose is calculated. For instance, the choice of using a dynamic bladder model and its voiding time may significantly affect the final dose. The doses for different voiding times are not systematically

reported but, for example, a faster voiding schedule would reduce the ED of ^{11}C-flumazenil by 13% (*5*) and that of ^{18}F-CP-18 by 61% (*6*).

Comparing the dose obtained by two different teams for the same tracer is a useful natural experiment to evaluate the weight of dose calculations approaches. In the literature there are 21 tracers for which human dosimetry has been estimated more than once by two different teams. In 18 of these, the ED was reported for both tracers. The average relative difference of these 18 tracers was 42% (Suppl Table 3). Only for three tracers the two teams found a dose difference smaller than 10%.

The dose to the target organ is estimated even more variably than the ED. For organs that can void their content, the dose is largely dependent on the voiding parameters simulated in the study. To take the tracers above described, a faster bladder voiding reduced the dose to the bladder by 33% for ^{11}C-flumazenil (*5*) and by 74% for ^{18}F-CP-18 (*6*). Similarly, the dose to the gallbladder, the target organ for ^{18}F-fluortriopride, was reduced by 71% by a fatty meal (*7*). Among the 21 tracers with at least two dosimetry evaluations by different teams, in only 11 the two teams identified the same target organ, with an average relative difference in dose of 165% (and a median of 72%) (Suppl Table 3).

In summary, given their narrow variability around the mean value of 5 μSv/MBq, the dosimetry estimates reported in ^{11}C papers could be as different as the dose found for another ^{11}C tracer, had a different team performed the analysis or a different methodology to calculate the dose been used.

Among the animals used to extrapolate the human dose, monkeys are a better model than rodents, because they are more closely related to humans. Monkeys, however, are not widely available, are expensive, and require sophisticated medical monitoring.

We verified the agreement in terms of ED (Suppl Table 4) and target organ doses (Suppl Table 5) of 16 ^{11}C tracers and 21 ^{18}F tracers for which dosimetry from human and nonhuman primates was available. For both groups of tracers, monkey scans unpredictably under- or overestimated the human ED with a mean absolute percentage difference of 31%. Out of these 37 tracers, the target organ was reported for both species in 32. Out of these 32 pairs of studies, in only 11 the target organ was the same in both monkeys and humans, and the monkey dose poorly predicted the human dose (mean difference of 42 absolute percentage points). To highlight the impact of methodology in the outcome of dosimetry studies, the same team (or part of the same team) performed the calculations for both species in 9 of the 11 tracers where the target organ was the same, but the same team was responsible for 13 out of 21 studies in which the target organ was different.

Finally, we wish to make clear that we advocate abandoning dosimetry scans only for ^{11}C ligands, and not for isotopes with a longer half-life. The dosimetry (in humans) for ^{18}F tracers should be maintained, because they deliver a higher dose and have a higher variability (Figure 1). With the aim of reducing unnecessary exposure to the general public, we suggest nevertheless to use either the first-in-human protocol implemented at the NIH (*8*), which recommends dosimetry scans only for those tracers that prove to be successful, or the approach used at the Amsterdam University Medical Center, where only a single low-dose (74 MBq) ^{18}F whole-body scan is performed before proof-of-concept studies, in order to rule out abnormal tracer distributions. The dosimetry of more irradiating positron emitters, such as ^{89}Zr -whose dose is about two orders of magnitude higher than that of ^{11}C (*9,10*), should be calculated for each tracer before it can be employed.

Research support acknowledgment

This work was supported by the Intramural Research Program of the National Institute of Mental Health, National Institutes of Health (project number ZIAMH002852).

References

1. Parsey RV, Belanger MJ, Sullivan GM, et al. Biodistribution and radiation dosimetry of 11C-WAY100,635 in humans. *J Nucl Med.* 2005;46:614-619.

2. Hines CS, Liow J-S, Zanotti-Fregonara P, et al. Human biodistribution and dosimetry of 11C-CUMI-101, an agonist radioligand for serotonin-1A receptors in brain. *PloS one.* 2011;6:e25309.

3. Jiang H, Schmit NR, Koenen AR, et al. Safety, pharmacokinetics, metabolism and radiation dosimetry of (18)F-tetrafluoroborate ((18)F-TFB) in healthy human subjects. *EJNMMI Res.* 2017;7:90.

4. O'Doherty J, Jauregui-Osoro M, Brothwood T, et al. (18)F-Tetrafluoroborate, a PET Probe for Imaging Sodium/Iodide Symporter Expression: Whole-Body Biodistribution, Safety, and Radiation Dosimetry in Thyroid Cancer Patients. *J Nucl Med.* 2017;58:1666-1671.

5. Laymon CM, Narendran R, Mason NS, et al. Human biodistribution and dosimetry of the PET radioligand [(1)(1)C]flumazenil (FMZ). *Mol Imaging Biol.* 2012;14:115-122.

6. Doss M, Kolb HC, Walsh JC, et al. Biodistribution and radiation dosimetry of 18F-CP-18, a potential apoptosis imaging agent, as determined from PET/CT scans in healthy volunteers. *J Nucl Med.* 2013;54:2087-2092.

7. Doot RK, Dubroff JG, Scheuermann JS, et al. Validation of gallbladder absorbed radiation dose reduction simulation: human dosimetry of [(18)F]fluortriopride. *EJNMMI Phys.* 2018;5:21.

8. Zanotti-Fregonara P, Lammertsma AA, Innis RB. Suggested pathway to assess radiation safety of 18 F-labeled PET tracers for first-in-human studies. *European journal of nuclear medicine and molecular imaging.* 2013;40:1781-1783.

9. O'Donoghue JA, Lewis JS, Pandit-Taskar N, et al. Pharmacokinetics, Biodistribution, and Radiation Dosimetry for 89Zr-Trastuzumab in Patients with Esophagogastric Cancer. *Journal of Nuclear Medicine.* 2018;59:161-166.

10. Pandit-Taskar N, O'Donoghue JA, Ruan S, et al. First-in-Human Imaging with 89Zr-Df-IAB2M Anti-PSMA Minibody in Patients with Metastatic Prostate Cancer: Pharmacokinetics, Biodistribution, Dosimetry, and Lesion Uptake. *Journal of Nuclear Medicine.* 2016;57:1858-1864.

Figure 1

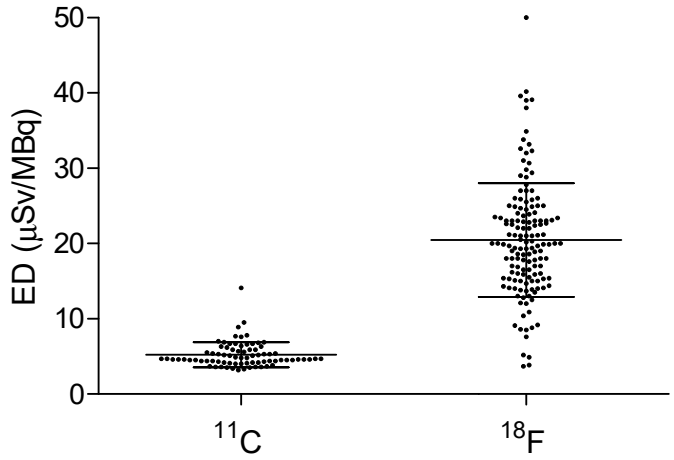

Scatterplots showing the estimation of human dose estimated for ^{11}C tracers (n =77) and for ^{18}F tracers (n = 144). The dose of ^{11}C tracers is about one fourth the dose of ^{18}F tracers, and its variability lower.

Supplemental Table 1: Human doses from ^{11}C-labeled tracers.

Target	Tracer	ED (µSV/MBq)	Critical organ	Critical organ dose (µSV/MBq)	Number of subjects	Reference
Acetylcholinesterase	Donepezil	5.2	Pancreas	27.1	6	(*1*)
Adenosine A1 receptor	MPDX	3.5	Liver	11	3	(*2*)
Adenosine A2A receptors	Preladenant	3.7	Gallbladder	17	5	(*3*)
Adenosine A2A receptors	TMSX	3.6	Liver/ Gallbladder	11	3	(*2*)
Amino acid transport	MeAIB	4	Pancreas	18	25	(*4*)
Antiglycemic drug	Metformin	9.5	Bladder	134	4	(*5*)
Beta amyloid	BTA1	4.3	Liver	20.1	5	(*6*)
Beta amyloid	Pib	4.7	Gallbladder	41.5	16	(*7*)
Beta amyloid	Pib	5.3	Gallbladder	44.8	6	(*8*)
Butyrylcholinesterase	MP4B	4.2	Kidney	13.7	7	(*9*)
Cannabinoid CB1 receptors	MePPEP	4.6	Liver	16.2	7	(*10*)
Cannabinoid CB2 receptors	NE40	3.6	Small intestine	15.6	6	(*11*)
Central adrenoceptors	Mirtazapine	6.8	Lungs	34	1	(*12*)
Cholestatic disease	Cholylsarcosine	6.2	Gallbladder	179.9	8	(*13*)
COX-1	PS13	4.6	Spleen	27.8	15	NIMH data
COX-2	MC1	4.6	Liver	18	2	NIMH data
Dopamine D1 receptors	NNC112	5.7	Gallbladder	32.4	7	(*14*)
Dopamine D2 receptors	Raclopride	6.3	Gallbladder	31.5	6	(*15*)
Dopamine D2 receptors	Raclopride	6.7	Kidneys	40.6	3	(*16*)
Dopamine D2/D3 receptors	PHNO	4.5	Liver	17.9	6	(*17*)
Dopamine system	NPA	6.7	Gallbladder	28.1	6	(*18*)
Dopamine transporters	PE2I	6.4	Bladder	18	3	(*19*)

Dopamine transporters	CFT	8.9	Bladder	63.2	6	(*20*)
Epidermal growth factor receptor	PD153035	4.7	Bladder	60.8	9	(*21*)
Extrastriatal dopamine D_2 receptor	FLB 457	5.9	Kidney	17.1	6	(*22*)
Fatty acid amide hydrolase	Carbonyl-URB694	4.6	Gallbladder	111	6	(*23*)
Fatty acids metabolism	Palmitate	3.2	Liver	27.5	2	(*24*)
GABA receptors	MPGA	4.8	Small intestine	33	3	(*25*)
GABA receptors	Flumazenil	5.2	Bladder	36.8	5	(*26*)
GABA receptors	Flumazenil	7.6	Bladder	63.2	6	(*27*)
Glucose metabolism	Glucose	4.3 [a]	Brain	11.6	33	(*28*)
Glycine transporter 1	RO5013853	3.3	Liver	16	3	(*29*)
Glycine transporter 1	GSK931145	4.5	Liver	11.5	8	(*30*)
H3 receptors	MK-8278	5.4	Pancreas	40.2	3	(*31*)
Histamine H3 receptors	TASP457	6.9	Pancreas	27.4	3	(*32*)
Imidazoline2 binding site	BU99008	5.6	Heart	28	4	(*33*)
Infection imaging	Trimethoprim	4.4	Kidney	14.5	3	(*34*)
mGlu1 receptors	ITMM	4.4	Bladder	12.5	12	(*35*)
mGlu1 receptors	ITMM	4.6	Bladder	13.2	3	(*36*)
mGlu2 receptors	JNJ-42491293	4.5	N/A	N/A	3	(*37*)
mGlu5 receptors	ABP688	3.7 [a]	Liver	16.4	5	(*38*)
mGlu5 receptors	FPEB	3.7	Gallbladder	41.2	6	(*39*)
mGlu5 receptors	SP203	4.4	Gallbladder	38.1	8	(*39*)
Mu-opiate receptors	Carfentanil	4.6	Bladder	36.5	5	(*40*)
Neuroinflammation	Ketoprofen	4.7	Bladder	41	6	(*41*)
Nicotine	Nicotine	5.4	Bladder	14.7	11	(*42*)
Nicotinic acetylcholine receptors	CHIBA-1001	6.9	Small intestine	24	3	(*43*)
NMDA receptors	GMOM	4.5	Spleen	12.7	5	(*44*)
NMDA receptors	CNS5161	10.6 [a]	Lungs	39.3	5	(*45*)

NOP1 receptors	NOP1	4.3	Gallbladder	21	9	(*46*)
OATP1B3	Telmisartan	4.2	Gallbladder	41.6	6	(*47*)
P2X7 receptor	JNJ54173717	4.5	Gallbladder	25	3	(*48*)
P-glycoprotein	dLop	7.8	Kidney	50.1	8	(*49*)
P-glycoprotein	Elacridar	3.4	Liver	27.6	3	(*50*)
P-glycoprotein	Tariquidar	3.6	Liver	31.9	3	(*50*)
P-glycoprotein	Laniquidar	4.4	Liver	25	6	(*51*)
Phosphodiesterase 4	Rolipram	4.8	Gallbladder	23.1	8	(*52*)
Serotonin 1A receptors	WAY-100635	14.1	Bladder	194	6	(*53*)
Serotonin 1A receptors	CUMI-101	5.3	Pancreas	32	9	(*54*)
Serotonin 2A receptors	Cimbi-36	5.5	Spleen	18.4	5	(*55*)
Serotonin 2A receptors	Cimbi-36_5	5.3	Spleen	17.9	2	(*55*)
Serotonin 6 receptors	GSK215083	7.7	Lungs	25.6	6	(*56*)
Serotonin transporters	Dasb	7	Lungs	32.8	7	(*57*)
Sigma receptors	SA4503	6.7	Spleen/ Thyroid	24	3	(*2*)
Synaptic density	UCB-J	7.6	Bladder (males) Liver (females)	22.4; 24.8	4	(*58*)
TSPO protein	PBR28	6.6	Kidney	52.6	7	(*59*)
TSPO protein	PK11195	5.1	Kidney	14	5	(*60*)
TSPO protein	PK11195	4.6 [a]	Bladder	12	7	(*61*)
TSPO protein	CB184	5.9	Kidney	21	5	(*62*)
TSPO protein	DPA-713	5.9	Lungs	20.1	6	(*63*)
TSPO protein	DAA1106	4.1	Spleen	18.2	12	(*64*)
TSPO protein	ER176	4.1	Kidney	14.3	9	(*65*)
Tumor imaging	Methyl-thymidine	3.8	Liver	37	6	(*66*)
Tumor imaging	Choline	4.4	Kidney	21	6	(*67*)
Tumor imaging	Docetaxel	4.7	Liver	35.2	5	(*68*)
Tumor imaging	Acetate	4.9	Pancreas	17	6	(*69*)
Tumor imaging	Acetate	3.5	Kidney	52	14	(*70*)
Tumor imaging	Methionine	5.1	Bladder	27	5	(*71*)
Tumor imaging	Erlotinib	3.6	Liver	29.4	1	(*72*)

Tumor imaging	Methyl-L-Cysteine	4.0	Liver	10.1	6	(*73*)
Tumor imaging	4DST	4.2	Bladder	17.6	3	(*74*)

When separate doses for men and women or for different ethnicities are reported, the average value was used. Doses to children were not considered.

[a] Effective dose equivalent (EDE). Tracers for which the dosimetry is expressed as EDE are not included in the mean ± SD of the tracer doses, nor in Figure 1

References

1. Gjerloff T, Jakobsen S, Nahimi A, et al. In vivo imaging of human acetylcholinesterase density in peripheral organs using 11C-donepezil: dosimetry, biodistribution, and kinetic analyses. *J Nucl Med.* 2014;55:1818-1824.

2. Sakata M, Oda K, Toyohara J, Ishii K, Nariai T, Ishiwata K. Direct comparison of radiation dosimetry of six PET tracers using human whole-body imaging and murine biodistribution studies. *Ann Nucl Med.* 2013;27:285-296.

3. Sakata M, Ishibashi K, Imai M, et al. Initial Evaluation of an Adenosine A2A Receptor Ligand, (11)C-Preladenant, in Healthy Human Subjects. *J Nucl Med.* 2017;58:1464-1470.

4. Tolvanen T, Nagren K, Yu M, et al. Human radiation dosimetry of [11C]MeAIB, a new tracer for imaging of system A amino acid transport. *Eur J Nucl Med Mol Imaging.* 2006;33:1178-1184.

5. Gormsen LC, Sundelin EI, Jensen JB, et al. In Vivo Imaging of Human 11C-Metformin in Peripheral Organs: Dosimetry, Biodistribution, and Kinetic Analyses. *J Nucl Med.* 2016;57:1920-1926.

6. Thees S, Neumaier B, Glatting G, et al. Radiation dosimetry and biodistribution of the beta-amyloid plaque imaging tracer 11C-BTA-1 in humans. *Nuklearmedizin.* 2007;46:175-180.

7. Scheinin NM, Tolvanen TK, Wilson IA, Arponen EM, Nagren KA, Rinne JO. Biodistribution and radiation dosimetry of the amyloid imaging agent 11C-PIB in humans. *J Nucl Med.* 2007;48:128-133.

8. O'Keefe GJ, Saunder TH, Ng S, et al. Radiation dosimetry of beta-amyloid tracers 11C-PiB and 18F-BAY94-9172. *J Nucl Med.* 2009;50:309-315.

9. Virta JR, Tolvanen T, Nagren K, Bruck A, Roivainen A, Rinne JO. 1-11C-methyl-4-piperidinyl-N-butyrate radiation dosimetry in humans by dynamic organ-specific evaluation. *J Nucl Med.* 2008;49:347-353.

10. Terry GE, Hirvonen J, Liow JS, et al. Biodistribution and dosimetry in humans of two inverse agonists to image cannabinoid CB1 receptors using positron emission tomography. *Eur J Nucl Med Mol Imaging.* 2010;37:1499-1506.

11. Ahmad R, Koole M, Evens N, et al. Whole-body biodistribution and radiation dosimetry of the cannabinoid type 2 receptor ligand [11C]-NE40 in healthy subjects. *Mol Imaging Biol.* 2013;15:384-390.

12. Marthi K, Hansen SB, Jakobsen S, Bender D, Smith SB, Smith DF. Biodistribution and radiation dosimetry of [N-methyl-11C]mirtazapine, an antidepressant affecting adrenoceptors. *Appl Radiat Isot.* 2003;59:175-179.

13. Frisch K, Kjaergaard K, Horsager J, Schacht AC, Munk OL. Human biodistribution, dosimetry, radiosynthesis and quality control of the bile acid PET tracer [N-methyl-(11)C]cholylsarcosine. *Nucl Med Biol.* 2019;72-73:55-61.

14. Cropley VL, Fujita M, Musachio JL, et al. Whole-body biodistribution and estimation of radiation-absorbed doses of the dopamine D1 receptor radioligand 11C-NNC 112 in humans. *J Nucl Med.* 2006;47:100-104.

15. Slifstein M, Hwang DR, Martinez D, et al. Biodistribution and radiation dosimetry of the dopamine D2 ligand 11C-raclopride determined from human whole-body PET. *J Nucl Med.* 2006;47:313-319.

16. Ribeiro MJ, Ricard M, Bourgeois S, et al. Biodistribution and radiation dosimetry of [11C]raclopride in healthy volunteers. *Eur J Nucl Med Mol Imaging.* 2005;32:952-958.

17. Mizrahi R, Rusjan P, Vitcu I, et al. Whole-body distribution and radiation dosimetry of 11C-(+)-PHNO, a D2/3 agonist ligand. *J Nucl Med.* 2012;53:1802-1806.

18. Laymon CM, Mason NS, Frankle WG, et al. Human biodistribution and dosimetry of the D2/3 agonist 11C-N-propylnorapomorphine (11C-NPA) determined from PET. *J Nucl Med.* 2009;50:814-817.

19. Ribeiro MJ, Ricard M, Lievre MA, et al. Whole-body distribution and radiation dosimetry of the dopamine transporter radioligand [(11)C]PE2I in healthy volunteers. *Nucl Med Biol.* 2007;34:465-470.

20. Huang T, Wang H, Tang G, et al. Human radiation dose estimation of (11)C-CFT using whole-body PET. *Clin Nucl Med.* 2012;37:1159-1162.

21. Liu N, Li M, Li X, et al. PET-based biodistribution and radiation dosimetry of epidermal growth factor receptor-selective tracer 11C-PD153035 in humans. *J Nucl Med.* 2009;50:303-308.

22. Kimura Y, Ito H, Shiraishi T, et al. Biodistribution and radiation dosimetry in humans of [(1)(1)C]FLB 457, a positron emission tomography ligand for the extrastriatal dopamine D(2) receptor. *Nucl Med Biol.* 2014;41:102-105.

23. Boileau I, Bloomfield PM, Rusjan P, et al. Whole-body radiation dosimetry of 11C-carbonyl-URB694: a PET tracer for fatty acid amide hydrolase. *J Nucl Med.* 2014;55:1993-1997.

24. Christensen NL, Jakobsen S, Schacht AC, et al. Whole-Body Biodistribution, Dosimetry, and Metabolite Correction of [(11)C]Palmitate: A PET Tracer for Imaging of Fatty Acid Metabolism. *Mol Imaging.* 2017;16:1536012117734485.

25. Santens P, De Vos F, Thierens H, et al. Biodistribution and dosimetry of carbon-11-methoxyprogabidic acid, a possible ligand for GABA-receptors in the brain. *J Nucl Med.* 1998;39:307-310.

26. Nugent AC, Neumeister A, Drevets WC, Eckelman WC, Channing MA, Herscovitch P. Human biodistribution and dosimetry of the PET benzodiazepine receptor ligand 11C-flumazenil. *Journal of Nuclear Medicine.* 2004;45(suppl):434P.

27. Laymon CM, Narendran R, Mason NS, et al. Human biodistribution and dosimetry of the PET radioligand [(1)(1)C]flumazenil (FMZ). *Mol Imaging Biol.* 2012;14:115-122.

28. Graham MM, Peterson LM, Muzi M, et al. 1-[Carbon-11]-glucose radiation dosimetry and distribution in human imaging studies. *J Nucl Med.* 1998;39:1805-1810.

29. Wong DF, Ostrowitzki S, Zhou Y, et al. Characterization of [11C]RO5013853, a novel PET tracer for the glycine transporter type 1 (GlyT1) in humans. *Neuroimage.* 2013;75:282-290.

30. Bullich S, Slifstein M, Passchier J, et al. Biodistribution and radiation dosimetry of the glycine transporter-1 ligand 11C-GSK931145 determined from primate and human whole-body PET. *Mol Imaging Biol.* 2011;13:776-784.

31. Van Laere KJ, Sanabria-Bohorquez SM, Mozley DP, et al. (11)C-MK-8278 PET as a tool for pharmacodynamic brain occupancy of histamine 3 receptor inverse agonists. *J Nucl Med.* 2014;55:65-72.

32. Kimura Y, Seki C, Ikoma Y, et al. [(11)C]TASP457, a novel PET ligand for histamine H3 receptors in human brain. *Eur J Nucl Med Mol Imaging.* 2016;43:1653-1663.

33. Venkataraman AV, Keat N, Myers JF, et al. First evaluation of PET-based human biodistribution and radiation dosimetry of (11)C-BU99008, a tracer for imaging the imidazoline2 binding site. *EJNMMI Res.* 2018;8:71.

34. Doot R, Young A, Schubert E, et al. First-in-human biodistribution and dosimetry of [11C]trimethoprim. *Journal of Nuclear Medicine.* 2019;60:1642.

35. Ito K, Sakata M, Oda K, et al. Comparison of dosimetry between PET/CT and PET alone using (11)C-ITMM. *Australas Phys Eng Sci Med.* 2016;39:177-186.

36. Toyohara J, Sakata M, Oda K, et al. Initial human PET studies of metabotropic glutamate receptor type 1 ligand 11C-ITMM. *J Nucl Med.* 2013;54:1302-1307.

37. Leurquin-Sterk G, Celen S, Van Laere K, et al. What We Observe In Vivo Is Not Always What We See In Vitro: Development and Validation of 11C-JNJ-42491293, A Novel Radioligand for mGluR2. *J Nucl Med.* 2017;58:110-116.

38. Treyer V, Streffer J, Ametamey SM, et al. Radiation dosimetry and biodistribution of 11C-ABP688 measured in healthy volunteers. *Eur J Nucl Med Mol Imaging.* 2008;35:766-770.

39. Lohith TG, Tsujikawa T, Simeon FG, et al. Comparison of two PET radioligands, [(11)C]FPEB and [(11)C]SP203, for quantification of metabotropic glutamate receptor 5 in human brain. *J Cereb Blood Flow Metab.* 2017;37:2458-2470.

40. Newberg AB, Ray R, Scheuermann J, et al. Dosimetry of 11C-carfentanil, a micro-opioid receptor imaging agent. *Nucl Med Commun.* 2009;30:314-318.

41. Ohnishi A, Senda M, Yamane T, et al. Human whole-body biodistribution and dosimetry of a new PET tracer, [(11)C]ketoprofen methyl ester, for imagings of neuroinflammation. *Nucl Med Biol.* 2014;41:594-599.

42. Garg PK, Lokitz SJ, Nazih R, Garg S. Biodistribution and Radiation Dosimetry of (11)C-Nicotine from Whole-Body PET Imaging in Humans. *J Nucl Med.* 2017;58:473-478.

43. Sakata M, Wu J, Toyohara J, et al. Biodistribution and radiation dosimetry of the alpha7 nicotinic acetylcholine receptor ligand [11C]CHIBA-1001 in humans. *Nucl Med Biol.* 2011;38:443-448.

44. van der Aart J, van der Doef TF, Horstman P, et al. Human Dosimetry of the N-Methyl-d-Aspartate Receptor Ligand (11)C-GMOM. *J Nucl Med.* 2017;58:1330-1333.

45. Dhawan V, Robeson W, Bjelke D, et al. Human Radiation Dosimetry for the N-Methyl-D-Aspartate Receptor Radioligand 11C-CNS5161. *J Nucl Med.* 2015;56:869-872.

46. Lohith TG, Zoghbi SS, Morse CL, et al. Brain and whole-body imaging of nociceptin/orphanin FQ peptide receptor in humans using the PET ligand 11C-NOP-1A. *J Nucl Med.* 2012;53:385-392.

47. Shimizu K, Takashima T, Yamane T, et al. Whole-body distribution and radiation dosimetry of [11C]telmisartan as a biomarker for hepatic organic anion transporting polypeptide (OATP) 1B3. *Nucl Med Biol.* 2012;39:847-853.

48. Van Weehaeghe D, Koole M, Schmidt ME, et al. [(11)C]JNJ54173717, a novel P2X7 receptor radioligand as marker for neuroinflammation: human biodistribution, dosimetry, brain kinetic modelling and quantification of brain P2X7 receptors in patients with Parkinson's disease and healthy volunteers. *Eur J Nucl Med Mol Imaging.* 2019;46:2051-2064.

49. Seneca N, Zoghbi SS, Liow JS, et al. Human brain imaging and radiation dosimetry of 11C-N-desmethyl-loperamide, a PET radiotracer to measure the function of P-glycoprotein. *J Nucl Med.* 2009;50:807-813.

50. Bauer M, Blaickner M, Philippe C, et al. Whole-Body Distribution and Radiation Dosimetry of 11C-Elacridar and 11C-Tariquidar in Humans. *J Nucl Med.* 2016;57:1265-1268.

51. Postnov A, Froklage FE, van Lingen A, et al. Radiation dose of the P-glycoprotein tracer 11C-laniquidar. *J Nucl Med.* 2013;54:2101-2103.

52. Sprague DR, Fujita M, Ryu YH, Liow JS, Pike VW, Innis RB. Whole-body biodistribution and radiation dosimetry in monkeys and humans of the phosphodiesterase 4 radioligand [(11)C](R)-rolipram: comparison of two-dimensional planar, bisected and quadrisected image analyses. *Nucl Med Biol.* 2008;35:493-500.

53. Parsey RV, Belanger MJ, Sullivan GM, et al. Biodistribution and radiation dosimetry of 11C-WAY100,635 in humans. *J Nucl Med.* 2005;46:614-619.

54. Hines CS, Liow J-S, Zanotti-Fregonara P, et al. Human biodistribution and dosimetry of 11C-CUMI-101, an agonist radioligand for serotonin-1A receptors in brain. *PloS one.* 2011;6:e25309.

55. Johansen A, Holm S, Dall B, et al. Human biodistribution and radiation dosimetry of the 5-HT2A receptor agonist Cimbi-36 labeled with carbon-11 in two positions. *EJNMMI Res.* 2019;9:71.

56. Comley RA, Salinas C, Mizrahi R, et al. Biodistribution and radiation dosimetry of the serotonin 5-HT(6) ligand [(1)(1)C]GSK215083 determined from human whole-body PET. *Mol Imaging Biol.* 2012;14:517-521.

57. Lu JQ, Ichise M, Liow JS, Ghose S, Vines D, Innis RB. Biodistribution and radiation dosimetry of the serotonin transporter ligand 11C-DASB determined from human whole-body PET. *J Nucl Med.* 2004;45:1555-1559.

58. Bini J, Holden D, Fontaine K, et al. Human adult and adolescent biodistribution and dosimetry of the synaptic vesicle glycoprotein 2A radioligand 11C-UCB-J. *EJNMMI Research.* 2020;10:83.

59. Brown AK, Fujita M, Fujimura Y, et al. Radiation dosimetry and biodistribution in monkey and man of 11C-PBR28: a PET radioligand to image inflammation. *J Nucl Med.* 2007;48:2072-2079.

60. Hirvonen J, Roivainen A, Virta J, Helin S, Nagren K, Rinne JO. Human biodistribution and radiation dosimetry of 11C-(R)-PK11195, the prototypic PET ligand to image inflammation. *Eur J Nucl Med Mol Imaging.* 2010;37:606-612.

61. Kumar A, Muzik O, Chugani D, Chakraborty P, Chugani HT. PET-derived biodistribution and dosimetry of the benzodiazepine receptor-binding radioligand (11)C-(R)-PK11195 in children and adults. *J Nucl Med.* 2010;51:139-144.

62. Sakata M, Ishibashi K, Imai M, et al. Assessment of safety, efficacy, and dosimetry of a novel 18-kDa translocator protein ligand, [(11)C]CB184, in healthy human volunteers. *EJNMMI Res.* 2017;7:26.

63. Endres CJ, Coughlin JM, Gage KL, Watkins CC, Kassiou M, Pomper MG. Radiation dosimetry and biodistribution of the TSPO ligand 11C-DPA-713 in humans. *J Nucl Med.* 2012;53:330-335.

64. Brody AL, Okita K, Shieh J, et al. Radiation dosimetry and biodistribution of the translocator protein radiotracer [(11)C]DAA1106 determined with PET/CT in healthy human volunteers. *Nucl Med Biol.* 2014;41:871-875.

65. Ikawa M, Lohith TG, Shrestha S, et al. 11C-ER176, a Radioligand for 18-kDa Translocator Protein, Has Adequate Sensitivity to Robustly Image All Three Affinity Genotypes in Human Brain. *J Nucl Med.* 2017;58:320-325.

66. Thierens H, van Eijkeren M, Goethals P. Biokinetics and dosimetry for [methyl-11C]thymidine. *Br J Radiol.* 1994;67:292-295.

67. Tolvanen T, Yli-Kerttula T, Ujula T, et al. Biodistribution and radiation dosimetry of [(11)C]choline: a comparison between rat and human data. *Eur J Nucl Med Mol Imaging.* 2010;37:874-883.

68. van der Veldt AA, Hendrikse NH, Smit EF, et al. Biodistribution and radiation dosimetry of 11C-labelled docetaxel in cancer patients. *Eur J Nucl Med Mol Imaging.* 2010;37:1950-1958.

69. Seltzer MA, Jahan SA, Sparks R, et al. Radiation dose estimates in humans for (11)C-acetate whole-body PET. *J Nucl Med.* 2004;45:1233-1236.

70. Liu D, Khong PL, Gao Y, et al. Radiation Dosimetry of Whole-Body Dual-Tracer 18F-FDG and 11C-Acetate PET/CT for Hepatocellular Carcinoma. *J Nucl Med.* 2016;57:907-912.

71. Deloar HM, Fujiwara T, Nakamura T, et al. Estimation of internal absorbed dose of L-[methyl-11C]methionine using whole-body positron emission tomography. *Eur J Nucl Med.* 1998;25:629-633.

72. Petrulli JR, Hansen SB, Abourbeh G, et al. A multi species evaluation of the radiation dosimetry of [(11)C]erlotinib, the radiolabeled analog of a clinically utilized tyrosine kinase inhibitor. *Nucl Med Biol.* 2017;47:56-61.

73. Yao B, Tang C, Tang G, et al. Human Biodistribution and Radiation Dosimetry of S-11C-Methyl-L-Cysteine Using Whole-Body PET. *Clin Nucl Med.* 2015;40:e470-474.

74. Toyohara J, Nariai T, Sakata M, et al. Whole-body distribution and brain tumor imaging with (11)C-4DST: a pilot study. *J Nucl Med.* 2011;52:1322-1328.

Supplemental Table 2: Human doses from ^{18}F-labeled tracers.

Target	Tracer	ED (μSV/MBq)	Critical organ	Critical organ dose (μSV/MBq)	Number of subjects	Reference
Adenosine 2A receptor	MNI-444	23	ULI	99	4	(*1*)
Adenosine A1 receptor	CPFPX	17.6	Gallbladder	136.2	6	(*2*)
Amino acid transporter 1	NKO-035	20	Bladder	302	4	(*3*)
Amino acid transporter 1	BF3-Tyr	3.7	N/A	N/A	2	(*4*)
Apoptosis	F-ML-10	15.4	Bladder	172	8	(*5*)
Apoptosis	CP-18	38	Bladder	536	7	(*6*)
Beta amyloid	FPYBF-2	8.5	Liver	32.6	4	(*7*)
Beta amyloid	FC119S	3.9	N/A	N/A	3	(*8*)
Beta-amyloid	FACT	18.6	Gallbladder	333	6	(*9*)
Beta-amyloid	Flutemetamol (GE067)	33.8	Gallbladder	287	6	(*10*)
Beta-amyloid	Flutemetamol (GE067)	26	Bladder	114	6	(*11*)
Beta-amyloid	Florbetaben (BAY94-9172)	14.7	Gallbladder	132.4	3	(*12*)
Beta-amyloid	Florbetaben (BAY94-9172)	16.5	Gallbladder	103	12	(*13*)
Beta-amyloid	Florbetapir (AV-45)	16	Gallbladder	150	9	(*14*)
Beta-amyloid	Florbetapir (AV-45)	13	N/A	N/A	3	(*15*)
Beta-amyloid	Florbetapir (AV-45)	19.3	Gallbladder	184.7	3	(*16*)
Beta-amyloid	Florbetapir (AV-45)	18.6	Gallbladder	143	9	(*17*)
Beta-amyloid	Florbetapir (AV-45)	17.8	Gallbladder	28.9	6	(*18*)
Beta-secretase 1	PF-06684511	24.7	Pancreas	92.9	5	(*19*)
Bone imaging	FNA	17	Bladder	80	8	(*20*)
Boron neutron capture therapy	FBPA	23.9	Kidney	32	3	(*21*)
Boron neutron capture	FBPA	15	Heart	14	6	(*22*)

therapy						
Cannabinoid CB1 receptors	FMPEP-d2	19.7	Bladder	66.2	7	(*23*)
Cannabinoid CB1 receptors	MK-9470	22.8	Gallbladder	159	8	(*24*)
Cardiac sympathetic innervation	4F-MHPG	21.1	Bladder	175	4	(*25*)
Cardiac sympathetic innervation	3F-PHPG	20.3	Bladder	165	4	(*25*)
Caspase 3	ICMT-11	25	Gallbladder	594	8	(*26*)
c-Met receptor	AH113804	29.8	Bladder	351	6	(*27*)
Deoxycytidine kinase	Clofarabine	20	Bladder	234	5	(*28*)
Deoxycytidine kinase	L-18F-FMAC	9.1	Bladder	54.3	3	(*29*)
Deoxycytidine kinase	L-18F-FAC	7.6	Bladder	49.6	3	(*29*)
Deoxycytidine kinase	FAC	5.2	Bladder	20.4	3	(*29*)
Deoxycytidine kinase	FAC	13.7	Bladder	55.7	3	(*30*)
Dopamine D2/D3 receptors	Fallypride	21.1	Gallbladder	120	5	(*31*)
Dopamine D3 receptors	Fluortriopride	22.5	Gallbladder	436	10	(*32*)
Dopamine transporters	FE-PE2I	23	Bladder	119	5	(*33*)
Dopamine transporters	FP-CIT	8.6 [a]	Bladder	58.6	12	(*34*)
Dopaminergic system	FDOPA	19.9	Bladder	150	18	(*35*)
Estrogen receptors	16α-F-estradiol	27	Gallbladder	797	10	(*36*)
Estrogen receptors	16α-F-estradiol	22 [b]	Liver	126	49	(*37*)
Fatty acids metabolism	fluoropivalate	15.4	Liver	70.6	24	(*38*)
Fatty acids metabolism	FluorBetaOx	14	Bladder	110	8	(*39*)
Folate receptor alpha	AzaFol	18	Liver	51.9	6	(*40*)
Gastrin-Releasing Peptide receptor	BAY 864367	23	Gallbladder	240	5	(*41*)
Gastrin-Releasing Peptide receptor	BAY 864367	14.3	Bladder	49.9	10	(*42*)
Gene expression	FHBG	15.9	Bladder	94.2	10	(*43*)

Glucose metabolism	FDG	29	Bladder	310	6	(*44*)
Glucose metabolism	FDG	24 [c]	Bladder	73	24 [d]	(*45*)
Glucose metabolism	FDG	15	Bladder	52	30	(*46*)
Glucose metabolism	FDG	15.3	Bladder	84.6	8	(*47*)
Glucose metabolism	FDG	19.9	Bladder	154	183	(*48*)
Glycine transporter 1	CFpyPB (MK-6577)	24.5	Gallbladder	267	3	(*49*)
Glycoprotein IIb/IIIa receptors	GP1	21.2	Bladder	88.4	30	(*50*)
Histone deacetylase 6	EKZ-001	39.1	Upper large intestine	270	4	(*51*)
Hypoxia	FMISO	14 [b]	Bladder	29	60	(*52*)
Hypoxia	FETNIM	19	Bladder	127	27	(*53*)
Hypoxia	EF5	18	Bladder	120	16	(*54*)
Hypoxia	EF5	23	Bladder	170	10	(*55*)
Hypoxia	DiFA	14.4	Bladder	94.7	8	(*56*)
Hypoxia	FAZA	13.5	Bladder	47	5	(*57*)
Hypoxia	HX4	27	Bladder	299	4	(*58*)
Infection imaging	Fluorodeoxysorbitol	21	Bladder	248	6	(*59*)
Integrins	Galacto-RGD	18	Bladder	200	5	(*60*)
Integrins	RGD-K5	31	Bladder	376	4	(*61*)
Integrins	FPPRGD2	39.6	Bladder	233.3	5	(*62*)
Melanoma imaging	P3BZA	19.3	Bladder	120	6	(*63*)
mGlu1 receptors	FIMX	23.4	Bladder	251	4	(*64*)
mGlu5 receptors	SP203	17.8	Bladder	76	7	(*65*)
mGlu5 receptors	PSS232	15.3	Gallbladder	23	6	(*66*)
mGlu5 receptors	FPEB	25	Bladder	258	9	(*67*)
mGlu5 receptors	FPEB	16.9	Gallbladder	191	6	(*68*)
Mitochondria	FBnTP	27	Liver	128	3	(*69*)
Muscarinic receptors	F-DEX	19.7	Liver	52.9	5	(*70*)
Myocardial perfusion	Flurpiridaz (BMS-747158)	19	Kidney	66	13	(*71*)
Myocardial perfusion	BFPET	18	Kidney	N/A	6	(*72*)

Neuroendocrine tumors	MFBG	23	Bladder	186	10	(*73*)
Nicotinic acetylcholine receptor	nifene	24.9	Bladder	179.7	4	(*74*)
Nicotinic acetylcholine receptors	A-85380	19.4	Bladder	81.8	3	(*75*)
Nicotinic acetylcholine receptors	A-85380	39	Bladder	180	6	(*76*)
Nicotinic acetylcholine receptors	A-85380	23.7	Bladder	153	2	(*77*)
Nicotinic acetylcholine receptors	flubatine	23.4	Bladder	80.2	3	(*78*)
Nicotinic acetylcholine receptors	AZAN	14	Bladder	23	2	(*79*)
Nicotinic acetylcholine receptors	NCFHEB	22.9	Bladder	80.2	3	(*80*)
Nitric oxide synthase	NOS	15.9	Bladder	95.3	16	(*81*)
Norepinephrine transporter	LMI1195	26	Bladder	101.5	12	(*82*)
Norepinephrine transporter	FMeNER-D2	17	Bladder	38	4	(*83*)
O-GlcNAcase	LSN3316612	20.5	Bladder	86.4	6	(*84*)
P2X7 receptor	JNJ-64413739	22	Gallbladder	256	3	(*85*)
Phosphodiesterase 10A	JNJ-42259152	24.9	Gallbladder	239	6	(*86*)
Phosphodiesterase 10A	MNI-659	24.1	Gallbladder	505	4	(*87*)
Phosphodiesterase 2A	PF-05270430	34.9	Gallbladder	N/A	4	(*88*)
Prostate cancer	F-choline	18 [e]	Kidney	79	10	(*89*)
Prostate cancer	F-choline	34.1 [b]	Kidney	170	12	(*90*)
Prostate cancer	FDHT	12.5 [a]	Bladder	86.8	7	(*91*)
Prostate cancer	FDHT	20	Bladder	61	11	(*92*)
Prostate cancer	DCFBC	19.9	Bladder	32.4	5	(*93*)
Prostate cancer	JK-PSMA-7	10.9	Kidney	17.6	10	(*94*)
Prostate cancer	PSMA-11	12.8	Bladder	126	6	(*95*)

Prostate cancer	CTT1057	23	Bladder	259	5	(*96*)
Prostate cancer	DCFPyL	17	Lacrimal glands	242	9	(*97*)
Prostate cancer	DCFPyL	13.9	Kidney	94.5	9	(*98*)
Prostate cancer	PSMA-1007	22	Kidney	170	3	(*99*)
Prostate cancer	FSU-880	9.2	Kidney	54.4	6	(*100*)
Prostate cancer	Florastamin	4.9	Kidney	62	15	(*101*)
Pyruvate kinase M2	DASA-23	23.5	Gallbladder	607.8	5	(*102*)
Serotonin 5-HT1A receptors	Mefway	40.2	Bladder	471	6	(*103*)
Sigma 1 receptors	Fluspidine	21	Liver	76	4	(*104*)
Sigma-1 receptors	FTC-146	25.9	Bladder	149.8	10	(*105*)
Sodium iodide symporter	tetrafluoroborate	50	Thyroid	31	8	(*106*)
Sodium iodide symporter	tetrafluoroborate	32.6	Thyroid	135	5	(*107*)
Somatostatin receptors	AIF-OC	22.4	Spleen	159	6	(*108*)
Somatostatin receptors	AIF-OC	23.1	Spleen	142	3	(*109*)
Tachykinin NK(1) receptors	SPA-RQ	32.3	Kidney	92	7	(*110*)
Tau protein	PI-2620	33.2	Right colon	242	6	(*111*)
Tau protein	AV1451 (T807)	22.5	Liver	81.2	6	(*112*)
Tau protein	GTP1	30.7	Gallbladder	14.1	6	(*113*)
Tau protein	MK-6240	29.4	Gallbladder	202	3	(*114*)
Tau protein	RO-948	15	Gallbladder	150	6	(*115*)
Tau protein	THK-5351	22.7	Gallbladder	242	12	(*116*)
Tau protein	JNJ-64326067	25.5	Right colon (males), bladder (females)	152, 182	6	(*117*)
TSPO	PBR06	18.5	Gallbladder	367	7	(*118*)
TSPO	FEPPA	20.2	Lungs	56.5	6	(*119*)
TSPO	DPA-714	21	Small intestine	47	6	(*120*)
Tumor imaging	5-fluorouracil	12.1	Gallbladder	79.9	15	(*121*)
Tumor imaging	FLT	15.5 [a]	Bladder	176.5	18	(*122*)
Tumor imaging	FACBC (GE-148) (fluciclovine)	14.1	Liver	52.2	6	(*123*)
Tumor imaging	FACBC (GE-148)	22.1	Pancreas	102.2	6	(*124*)

	(fluciclovine)					
Tumor imaging	FET	16.5	Bladder	60	7	(*125*)
Tumor imaging	fluoropaclitaxel	28.8	Gallbladder	229.5	3	(*126*)
Tumor imaging	fluoro-l-proline	15.1	Bladder	44.1	6	(*127*)
Tumor imaging	BAY 94-9392 (FSPG)	32	Bladder	400	5	(*128*)
Tumor imaging	FFNP	20	Gallbladder	113	12	(*129*)
Tumor imaging	ISO-1	16	Gallbladder	91	12	(*130*)
Tumor imaging	NMK36	13.8	Liver	40.6	6	(*131*)
Tumor imaging	SKI	25.8	Colon	167	5	(*132*)
Tumor imaging	(2S, 4R)4-fluoroglutamine	19.4	Uterus	54.9	6	(*133*)
Tumor imaging	(2S, 4R)4-fluoroglutamine	18.9	Bladder	186	6	(*134*)
Tumor imaging	FdCyd	21.2	Bladder	79.6	5	(*135*)
Tumor imaging	Fludarabine	10.4	Spleen	37.5	10	(*136*)
Tumor imaging	D4-FCH	25	Kidney	106	8	(*137*)
Tumor imaging	BAY 86-9596	16.2	N/A	N/A	5	(*138*)
Tumor imaging	FMP	13	N/A	N/A	5	(*139*)
Tumor imaging	BAY 85-8050 (TIM-1)	8.8	Kidney	25.3	5	(*140*)
Tumor imaging	FAPI-74	14.1	Bladder	75.8	10	(*141*)
Vesicular acetylcholine transporter	VAT	12	Gallbladder	104	3	(*142*)
Vesicular acetylcholine transporter	FEOBV	22.6	Upper large intestine	101	3	(*143*)
Vesicular monoamine transporter	FP-(+)-DTBZ	27.8	Pancreas	153.3	9	(*144*)

When separate doses for men and women or for different ethnicities are reported, the average value was used. Doses to children were not considered.

[a] Value estimated from the data reported in the original paper (estimations taken from (*65*))

[b] Effective dose equivalent (EDE). Tracers for which the dosimetry is expressed as EDE are not included in the mean ± SD of the tracer doses, nor in Figure 1

[c] Effective dose is estimated to be higher than total-body dose by approximately a factor of two (*45*).

[d] Residence times were calculated with a variable number of subjects pooled from different biodistribution studies (*45*).

[e] Risk-weighted absorbed dose coefficient

References

1. Barret O, Hannestad J, Vala C, et al. Characterization in humans of 18F-MNI-444, a PET radiotracer for brain adenosine 2A receptors. *J Nucl Med.* 2015;56:586-591.

2. Herzog H, Elmenhorst D, Winz O, Bauer A. Biodistribution and radiation dosimetry of the A1 adenosine receptor ligand 18F-CPFPX determined from human whole-body PET. *Eur J Nucl Med Mol Imaging.* 2008;35:1499-1506.

3. Watabe T, Naka S, Soeda F, et al. First in human dosimetry of 18F-NKO-035: a new PET probe targeting L-type amino acid transporter 1 (LAT1). *Journal of Nuclear Medicine.* 2020;61:627.

4. Li Z, Li J, Yang Z, Liu Z. Pilot Study of 18F-BF3-Tyr in Healthy Volunteers and Glioma Patients. *Journal of Nuclear Medicine.* 2020;61:1216.

5. Hoglund J, Shirvan A, Antoni G, et al. 18F-ML-10, a PET tracer for apoptosis: first human study. *J Nucl Med.* 2011;52:720-725.

6. Doss M, Kolb HC, Walsh JC, et al. Biodistribution and radiation dosimetry of 18F-CP-18, a potential apoptosis imaging agent, as determined from PET/CT scans in healthy volunteers. *J Nucl Med.* 2013;54:2087-2092.

7. Nishii R, Higashi T, Kagawa S, et al. (18)F-FPYBF-2, a new F-18 labelled amyloid imaging PET tracer: biodistribution and radiation dosimetry assessment of first-in-man (18)F-FPYBF-2 PET imaging. *Ann Nucl Med.* 2018;32:256-263.

8. Kim BI, Ha J-H, Lee KC, et al. First in human imaging of amyloid deposition in Alzheimer disease using the [18F]FC119S. *Journal of Nuclear Medicine.* 2013;54:1803.

9. Shidahara M, Tashiro M, Okamura N, et al. Evaluation of the biodistribution and radiation dosimetry of the 18F-labelled amyloid imaging probe [18F]FACT in humans. *EJNMMI Res.* 2013;3:32.

10. Koole M, Lewis DM, Buckley C, et al. Whole-body biodistribution and radiation dosimetry of 18F-GE067: a radioligand for in vivo brain amyloid imaging. *J Nucl Med.* 2009;50:818-822.

11. Senda M, Sasaki M, Fujikawa K, Paterson C, McParland B. Biodistribution and radiation dosimetry of Flutemetamol (18F) injection in Japanese healthy volunteers. *Journal of Nuclear Medicine.* 2012;53:1510.

12. O'Keefe GJ, Saunder TH, Ng S, et al. Radiation dosimetry of beta-amyloid tracers 11C-PiB and 18F-BAY94-9172. *J Nucl Med.* 2009;50:309-315.

13. Sattler B, Seese A, Barthel H, et al. Radiation risk caused by [F18]BAY 94-9172, a new PET tracer for detection of cerebral β-amyloid plaques. *Journal of Nuclear Medicine.* 2009;50:1840.

14. Adler L, Wolodzko J, Stabin M, McNelis T, Gammage L, Joshi A. Radiation dosimetry of F18-AV-45 measured by PET/CT in humans. *Journal of Nuclear Medicine.* 2008;49 (Suppl 1:283).

15. Wong DF, Rosenberg PB, Zhou Y, et al. In vivo imaging of amyloid deposition in Alzheimer disease using the radioligand 18F-AV-45 (florbetapir [corrected] F 18). *J Nucl Med.* 2010;51:913-920.

16. Lin KJ, Hsu WC, Hsiao IT, et al. Whole-body biodistribution and brain PET imaging with [18F]AV-45, a novel amyloid imaging agent--a pilot study. *Nucl Med Biol.* 2010;37:497-508.

17. Joshi AD, Pontecorvo MJ, Adler L, et al. Radiation dosimetry of florbetapir F 18. *EJNMMI Res.* 2014;4:4.

18. Nakano M, Nakamura T, Takita Y, et al. Radiation dosimetry and pharmacokinetics of florbetapir ((18)F) in Japanese subjects. *Ann Nucl Med.* 2019;33:639-645.

19. Arakawa R, Takano A, Stenkrona P, et al. PET imaging of beta-secretase 1 in the human brain: radiation dosimetry, quantification, and test-retest examination of [18F]PF-06684511. *European Journal of Nuclear Medicine and Molecular Imaging.* 2020.

20. Kurdziel KA, Shih JH, Apolo AB, et al. The kinetics and reproducibility of 18F-sodium fluoride for oncology using current PET camera technology. *J Nucl Med.* 2012;53:1175-1184.

21. Sakata M, Oda K, Toyohara J, Ishii K, Nariai T, Ishiwata K. Direct comparison of radiation dosimetry of six PET tracers using human whole-body imaging and murine biodistribution studies. *Ann Nucl Med.* 2013;27:285-296.

22. Kono Y, Kurihara H, Kawamoto H, et al. Radiation absorbed dose estimates for 18F-BPA PET. *Acta Radiol.* 2017;58:1094-1100.

23. Terry GE, Hirvonen J, Liow JS, et al. Biodistribution and dosimetry in humans of two inverse agonists to image cannabinoid CB1 receptors using positron emission tomography. *Eur J Nucl Med Mol Imaging.* 2010;37:1499-1506.

24. Van Laere K, Koole M, Sanabria Bohorquez SM, et al. Whole-body biodistribution and radiation dosimetry of the human cannabinoid type-1 receptor ligand 18F-MK-9470 in healthy subjects. *J Nucl Med.* 2008;49:439-445.

25. Raffel DM, Jung YW, Koeppe RA, et al. First-in-Human Studies of [(18)F] Fluorohydroxyphenethylguanidines. *Circ Cardiovasc Imaging.* 2018;11:e007965.

26. Challapalli A, Kenny LM, Hallett WA, et al. 18F-ICMT-11, a caspase-3-specific PET tracer for apoptosis: biodistribution and radiation dosimetry. *J Nucl Med.* 2013;54:1551-1556.

27. Somer EJ, Owenius R, Wall A, Antoni G, Thibblin A, Sorensen J. The clinical safety, biodistribution and internal radiation dosimetry of [(18)F]AH113804 in healthy adult volunteers. *EJNMMI Res.* 2016;6:87.

28. Barrio MJ, Spick C, Radu CG, et al. Human Biodistribution and Radiation Dosimetry of (18)F-Clofarabine, a PET Probe Targeting the Deoxyribonucleoside Salvage Pathway. *J Nucl Med.* 2017;58:374-378.

29. Schwarzenberg J, Radu CG, Benz M, et al. Human biodistribution and radiation dosimetry of novel PET probes targeting the deoxyribonucleoside salvage pathway. *Eur J Nucl Med Mol Imaging.* 2011;38:711-721.

30. Benz M, Radu C, Allen-Auerbach M, et al. Human biodistribution and dosimetry of the nucleoside analogue [18F]FAC in humans. *Journal of Nuclear Medicine.* 2008;49:284P.

31. Kessler RM, Mason NS, Jones C, Ansari MS, Manning RG, Price RR. [18F]N-allyl-5-fluoropropylepidepride (Fallypride): Radiation dosimetry. Quantification of striatal and extrastriatal dopamine receptors in man. *Neuroimage.* 2000;11:S32.

32. Doot RK, Dubroff JG, Scheuermann JS, et al. Validation of gallbladder absorbed radiation dose reduction simulation: human dosimetry of [(18)F]fluortriopride. *EJNMMI Phys.* 2018;5:21.

33. Lizana H, Johansson L, Axelsson J, et al. Whole-Body Biodistribution and Dosimetry of the Dopamine Transporter Radioligand (18)F-FE-PE2I in Human Subjects. *J Nucl Med.* 2018;59:1275-1280.

34. Robeson W, Dhawan V, Belakhlef A, et al. Dosimetry of the dopamine transporter radioligand 18F-FPCIT in human subjects. *J Nucl Med.* 2003;44:961-966.

35. Brown WD, Oakes TR, DeJesus OT, et al. Fluorine-18-fluoro-L-DOPA dosimetry with carbidopa pretreatment. *J Nucl Med.* 1998;39:1884-1891.

36. Beauregard JM, Croteau E, Ahmed N, van Lier JE, Benard F. Assessment of human biodistribution and dosimetry of 4-fluoro-11beta-methoxy-16alpha-18F-fluoroestradiol using serial whole-body PET/CT. *J Nucl Med.* 2009;50:100-107.

37. Mankoff DA, Peterson LM, Tewson TJ, et al. [18F]fluoroestradiol radiation dosimetry in human PET studies. *J Nucl Med.* 2001;42:679-684.

38. Dubash SR, Keat N, Kozlowski K, et al. Clinical translation of (18)F-fluoropivalate - a PET tracer for imaging short-chain fatty acid metabolism: safety, biodistribution, and dosimetry in fed and fasted healthy volunteers. *Eur J Nucl Med Mol Imaging.* 2020.

39. Laforest R, Delano D, Dence C, et al. PET/CT biodistribution and dosimetry of [18F]-FluorBetaOx in humans. *Journal of Nuclear Medicine.* 2013;54:1029.

40. Gnesin S, Muller J, Burger IA, et al. Radiation dosimetry of (18)F-AzaFol: A first in-human use of a folate receptor PET tracer. *EJNMMI Res.* 2020;10:32.

41. Smolarz K, Krause BJ, Schmelz Y, et al. Human biodistribution and radiation dosimetry of BAY 86-4367: A F-18 labeled bombesin antagonist for PET/CT imaging of prostate cancer. *Journal of Nuclear Medicine.* 2011;52:1456.

42. Sah BR, Burger IA, Schibli R, et al. Dosimetry and first clinical evaluation of the new 18F-radiolabeled bombesin analogue BAY 864367 in patients with prostate cancer. *J Nucl Med.* 2015;56:372-378.

43. Yaghoubi S, Barrio JR, Dahlbom M, et al. Human pharmacokinetic and dosimetry studies of [(18)F]FHBG: a reporter probe for imaging herpes simplex virus type-1 thymidine kinase reporter gene expression. *J Nucl Med.* 2001;42:1225-1234.

44. Deloar HM, Fujiwara T, Shidahara M, et al. Estimation of absorbed dose for 2-[F-18]fluoro-2-deoxy-D-glucose using whole-body positron emission tomography and magnetic resonance imaging. *Eur J Nucl Med.* 1998;25:565-574.

45. Hays MT, Watson EE, Thomas SR, Stabin M. MIRD dose estimate report no. 19: radiation absorbed dose estimates from (18)F-FDG. *J Nucl Med.* 2002;43:210-214.

46. Staaf J, Jacobsson H, Sanchez-Crespo A. A revision of the organ radiation doses from 2-fluoro-2-deoxy-D-glucose with reference to tumour presence. *Radiat Prot Dosimetry.* 2012;151:43-50.

47. Srinivasan S, Crandall JP, Gajwani P, et al. Human Radiation Dosimetry for Orally and Intravenously Administered 18F-FDG. *Journal of Nuclear Medicine.* 2020;61:613-619.

48. Quinn B, Dauer Z, Pandit-Taskar N, Schoder H, Dauer LT. Radiation dosimetry of 18F-FDG PET/CT: incorporating exam-specific parameters in dose estimates. *BMC Med Imaging.* 2016;16:41.

49. Joshi AD, Sanabria-Bohorquez SM, Bormans G, et al. Characterization of the novel GlyT1 PET tracer [18F]MK-6577 in humans. *Synapse.* 2015;69:33-40.

50. Lee N, Oh I, Chae SY, et al. Radiation dosimetry of [(18)F]GP1 for imaging activated glycoprotein IIb/IIIa receptors with positron emission tomography in patients with acute thromboembolism. *Nucl Med Biol.* 2019;72-73:45-48.

51. Koole M, Van Weehaeghe D, Serdons K, et al. Clinical validation of the novel HDAC6 radiotracer [18F]EKZ-001 in the human brain. *European Journal of Nuclear Medicine and Molecular Imaging.* 2020.

52. Graham MM, Peterson LM, Link JM, et al. Fluorine-18-fluoromisonidazole radiation dosimetry in imaging studies. *J Nucl Med.* 1997;38:1631-1636.

53. Tolvanen T, Lehtio K, Kulmala J, et al. 18F-Fluoroerythronitroimidazole radiation dosimetry in cancer studies. *J Nucl Med.* 2002;43:1674-1680.

54. Lin LL, Silvoniemi A, Stubbs JB, et al. Radiation dosimetry and biodistribution of the hypoxia tracer (1)(8)F-EF5 in oncologic patients. *Cancer Biother Radiopharm.* 2012;27:412-419.

55. Koch CJ, Scheuermann JS, Divgi C, et al. Biodistribution and dosimetry of (18)F-EF5 in cancer patients with preliminary comparison of (18)F-EF5 uptake versus EF5 binding in human glioblastoma. *Eur J Nucl Med Mol Imaging.* 2010;37:2048-2059.

56. Watanabe S, Shiga T, Hirata K, et al. Biodistribution and radiation dosimetry of the novel hypoxia PET probe [(18)F]DiFA and comparison with [(18)F]FMISO. *EJNMMI Res.* 2019;9:60.

57. Savi A, Incerti E, Fallanca F, et al. First Evaluation of PET-Based Human Biodistribution and Dosimetry of (18)F-FAZA, a Tracer for Imaging Tumor Hypoxia. *J Nucl Med.* 2017;58:1224-1229.

58. Doss M, Zhang JJ, Belanger MJ, et al. Biodistribution and radiation dosimetry of the hypoxia marker 18F-HX4 in monkeys and humans determined by using whole-body PET/CT. *Nucl Med Commun.* 2010;31:1016-1024.

59. Zhu W, Yao S, Xing H, et al. Biodistribution and Radiation Dosimetry of the Enterobacteriaceae-Specific Imaging Probe [(18)F]Fluorodeoxysorbitol Determined by PET/CT in Healthy Human Volunteers. *Mol Imaging Biol.* 2016;18:782-787.

60. Haubner R, Weber WA, Beer AJ, et al. Noninvasive visualization of the activated alphavbeta3 integrin in cancer patients by positron emission tomography and [18F]Galacto-RGD. *PLoS Med.* 2005;2:e70.

61. Doss M, Kolb HC, Zhang JJ, et al. Biodistribution and radiation dosimetry of the integrin marker 18F-RGD-K5 determined from whole-body PET/CT in monkeys and humans. *J Nucl Med.* 2012;53:787-795.

62. Mittra ES, Goris ML, Iagaru AH, et al. Pilot pharmacokinetic and dosimetric studies of (18)F-FPPRGD2: a PET radiopharmaceutical agent for imaging alpha(v)beta(3) integrin levels. *Radiology.* 2011;260:182-191.

63. Ma X, Wang S, Wang S, et al. Biodistribution, Radiation Dosimetry, and Clinical Application of a Melanin-Targeted PET Probe, (18)F-P3BZA, in Patients. *J Nucl Med.* 2019;60:16-22.

64. Zanotti-Fregonara P, Xu R, Zoghbi SS, et al. The PET Radioligand 18F-FIMX Images and Quantifies Metabotropic Glutamate Receptor 1 in Proportion to the Regional Density of Its Gene Transcript in Human Brain. *J Nucl Med.* 2016;57:242-247.

65. Kimura Y, Simeon FG, Hatazawa J, et al. Biodistribution and radiation dosimetry of a positron emission tomographic ligand, 18F-SP203, to image metabotropic glutamate subtype 5 receptors in humans. *Eur J Nucl Med Mol Imaging.* 2010;37:1943-1949.

66. Sah BR, Sommerauer M, Mu L, et al. Radiation dosimetry of [(18)F]-PSS232-a PET radioligand for imaging mGlu5 receptors in humans. *EJNMMI Res.* 2019;9:56.

67. Kessler RM, Seibyl J, Cowan RL, et al. Radiation Dosimetry of (18)F-FPEB in Humans. *J Nucl Med.* 2014;55:1119-1121.

68. Wong DF, Waterhouse R, Kuwabara H, et al. 18F-FPEB, a PET radiopharmaceutical for quantifying metabotropic glutamate 5 receptors: a first-in-human study of radiochemical safety, biokinetics, and radiation dosimetry. *J Nucl Med.* 2013;54:388-396.

69. Senthamizhchelvan S, Chaudhry M, Ravert H, et al. Human biodistribution and radiation dosimetry of 18F-fluorobenzyltriphenyl phosphonium. *Journal of Nuclear Medicine.* 2012;53:1512.

70. Pain CD, O'Keefe GJ, Ackermann U, Dore V, Villemagne VL, Rowe CC. Human biodistribution and internal dosimetry of 4-[18F]fluorobenzyl-dexetimide: a PET radiopharmaceutical for imaging muscarinic acetylcholine receptors in the brain and heart. *EJNMMI Research.* 2020;10:61.

71. Maddahi J, Czernin J, Lazewatsky J, et al. Phase I, first-in-human study of BMS747158, a novel 18F-labeled tracer for myocardial perfusion PET: dosimetry, biodistribution, safety, and imaging characteristics after a single injection at rest. *J Nucl Med.* 2011;52:1490-1498.

72. Elmaleh D, Kardan A, Barrow S, et al. A phase I study evaluating dosimetry and myocardial pharmacokinetic behavior of BFPET, a new F-18 labeled tracer for myocardial perfusion imaging. *Journal of Nuclear Medicine.* 2009;50:420.

73. Pandit-Taskar N, Zanzonico P, Staton KD, et al. Biodistribution and Dosimetry of (18)F-Meta-Fluorobenzylguanidine: A First-in-Human PET/CT Imaging Study of Patients with Neuroendocrine Malignancies. *J Nucl Med.* 2018;59:147-153.

74. Betthauser TJ, Hillmer AT, Lao PJ, et al. Human biodistribution and dosimetry of [(18)F]nifene, an alpha4beta2* nicotinic acetylcholine receptor PET tracer. *Nucl Med Biol.* 2017;55:7-11.

75. Bottlaender M, Valette H, Roumenov D, et al. Biodistribution and radiation dosimetry of 18F-fluoro-A-85380 in healthy volunteers. *J Nucl Med.* 2003;44:596-601.

76. Kimes AS, Horti AG, London ED, et al. 2-[^{18}F]F-A-85380: PET imaging of brain nicotinic acetylcholine receptors and whole body distribution in humans. *FASEB J.* 2003;17:1331-1333.

77. Obrzut SL, Koren AO, Mandelkern MA, Brody AL, Hoh CK, London ED. Whole-body radiation dosimetry of 2-[18F]Fluoro-A-85380 in human PET imaging studies. *Nucl Med Biol.* 2005;32:869-874.

78. Sattler B, Kranz M, Starke A, et al. Internal dose assessment of (-)-18F-flubatine, comparing animal model datasets of mice and piglets with first-in-human results. *J Nucl Med.* 2014;55:1885-1892.

79. Wong DF, Kuwabara H, Kim J, et al. PET imaging of high-affinity alpha4beta2 nicotinic acetylcholine receptors in humans with 18F-AZAN, a radioligand with optimal brain kinetics. *J Nucl Med.* 2013;54:1308-1314.

80. Sattler B, Wilke S, Starke A, et al. Radiation exposure by (-)-F18-NCFHEB, a new PET tracer for imaging of cerebral alpha4beta2 nicotinic acetylcholine receptors (nAChRs). *Journal of Nuclear Medicine.* 2011;52:1459.

81. Herrero P, Laforest R, Shoghi K, et al. Feasibility and dosimetry studies for 18F-NOS as a potential PET radiopharmaceutical for inducible nitric oxide synthase in humans. *J Nucl Med.* 2012;53:994-1001.

82. Sinusas AJ, Lazewatsky J, Brunetti J, et al. Biodistribution and radiation dosimetry of LMI1195: first-in-human study of a novel 18F-labeled tracer for imaging myocardial innervation. *J Nucl Med.* 2014;55:1445-1451.

83. Takano A, Halldin C, Varrone A, et al. Biodistribution and radiation dosimetry of the norepinephrine transporter radioligand (S,S)-[18F]FMeNER-D2: a human whole-body PET study. *Eur J Nucl Med Mol Imaging.* 2008;35:630-636.

84. Lee JH, Liow JS, Paul S, et al. PET quantification of brain O-GlcNAcase with [(18)F]LSN3316612 in healthy human volunteers. *EJNMMI Res.* 2020;10:20.

85. Koole M, Schmidt ME, Hijzen A, et al. (18)F-JNJ-64413739, a Novel PET Ligand for the P2X7 Ion Channel: Radiation Dosimetry, Kinetic Modeling, Test-Retest Variability, and Occupancy of the P2X7 Antagonist JNJ-54175446. *J Nucl Med.* 2019;60:683-690.

86. Van Laere K, Ahmad RU, Hudyana H, et al. Human biodistribution and dosimetry of 18F-JNJ42259152, a radioligand for phosphodiesterase 10A imaging. *Eur J Nucl Med Mol Imaging.* 2013;40:254-261.

87. Barret O, Thomae D, Tavares A, et al. In vivo assessment and dosimetry of 2 novel PDE10A PET radiotracers in humans: 18F-MNI-659 and 18F-MNI-654. *J Nucl Med.* 2014;55:1297-1304.

88. Constantinescu C, Cole P, Brown T, et al. Radiation dosimetry and biodistribution of [18F]PF-05270430, a radiotracer for phosphodiesterase 2A (PDE2A) in rhesus macaques and humans. *Journal of Nuclear Medicine.* 2018;59:1012.

89. Giussani A, Janzen T, Uusijarvi-Lizana H, et al. A compartmental model for biokinetics and dosimetry of 18F-choline in prostate cancer patients. *J Nucl Med.* 2012;53:985-993.

90. DeGrado TR, Reiman RE, Price DT, Wang S, Coleman RE. Pharmacokinetics and radiation dosimetry of 18F-fluorocholine. *J Nucl Med.* 2002;43:92-96.

91. Zanzonico PB, Finn R, Pentlow KS, et al. PET-based radiation dosimetry in man of 18F-fluorodihydrotestosterone, a new radiotracer for imaging prostate cancer. *J Nucl Med.* 2004;45:1966-1971.

92. McCall K, Abbott A, Hu J, et al. Report on the PET/CT image-based radiation dosimetry of 18FDHT in women, an imaging agent with new applications for evaluation of androgen receptor status in patients with metastatic breast cancer. *Journal of Nuclear Medicine.* 2019;60:1630.

93. Cho SY, Gage KL, Mease RC, et al. Biodistribution, tumor detection, and radiation dosimetry of 18F-DCFBC, a low-molecular-weight inhibitor of prostate-specific membrane antigen, in patients with metastatic prostate cancer. *J Nucl Med.* 2012;53:1883-1891.

94. Hohberg M, Kobe C, Krapf P, et al. Biodistribution and radiation dosimetry of [(18)F]-JK-PSMA-7 as a novel prostate-specific membrane antigen-specific ligand for PET/CT imaging of prostate cancer. *EJNMMI Res.* 2019;9:66.

95. Piron S, De Man K, Van Laeken N, et al. Radiation Dosimetry and Biodistribution of (18)F-PSMA-11 for PET Imaging of Prostate Cancer. *J Nucl Med.* 2019;60:1736-1742.

96. Behr SC, Aggarwal R, VanBrocklin HF, et al. Phase I Study of CTT1057, an (18)F-Labeled Imaging Agent with Phosphoramidate Core Targeting Prostate-Specific Membrane Antigen in Prostate Cancer. *J Nucl Med.* 2019;60:910-916.

97. Plyku D, Mena E, Rowe SP, et al. Combined model-based and patient-specific dosimetry for (18)F-DCFPyL, a PSMA-targeted PET agent. *Eur J Nucl Med Mol Imaging.* 2018;45:989-998.

98. Szabo Z, Mena E, Rowe SP, et al. Initial Evaluation of [(18)F]DCFPyL for Prostate-Specific Membrane Antigen (PSMA)-Targeted PET Imaging of Prostate Cancer. *Mol Imaging Biol.* 2015;17:565-574.

99. Giesel FL, Hadaschik B, Cardinale J, et al. F-18 labelled PSMA-1007: biodistribution, radiation dosimetry and histopathological validation of tumor lesions in prostate cancer patients. *Eur J Nucl Med Mol Imaging.* 2017;44:678-688.

100. Saga T, Nakamoto Y, Ishimori T, et al. Initial evaluation of PET/CT with 18F-FSU-880 targeting prostate-specific membrane antigen in prostate cancer patients. *Cancer Science.* 2019;110:742-750.

101. Lee I, Lim I, Byun BH, et al. A microdose clinical trial to evaluate [18F]Florastamin as a positron emission tomography imaging agent in patients with prostate cancer. *European Journal of Nuclear Medicine and Molecular Imaging.* 2020.

102. Beinat C, Patel CB, Haywood T, et al. Human biodistribution and radiation dosimetry of [(18)F]DASA-23, a PET probe targeting pyruvate kinase M2. *Eur J Nucl Med Mol Imaging.* 2020.

103. Choi JY, Lyoo CH, Kim JS, Kim KM, Lee M, Ryu YH. Biodistribution and Radiation Dosimetry of [(18)F]Mefway in Humans. *Mol Imaging Biol.* 2016;18:803-806.

104. Sattler B, Kranz M, Wuest N, et al. First-in-man incorporation dosimetry of (S)-(-)-[18F]fluspidine. *Journal of Nuclear Medicine.* 2016;57:1022.

105. Hjornevik T, Cipriano PW, Shen B, et al. Biodistribution and Radiation Dosimetry of (18)F-FTC-146 in Humans. *J Nucl Med.* 2017;58:2004-2009.

106. Jiang H, Schmit NR, Koenen AR, et al. Safety, pharmacokinetics, metabolism and radiation dosimetry of (18)F-tetrafluoroborate ((18)F-TFB) in healthy human subjects. *EJNMMI Res.* 2017;7:90.

107. O'Doherty J, Jauregui-Osoro M, Brothwood T, et al. (18)F-Tetrafluoroborate, a PET Probe for Imaging Sodium/Iodide Symporter Expression: Whole-Body Biodistribution, Safety, and Radiation Dosimetry in Thyroid Cancer Patients. *J Nucl Med.* 2017;58:1666-1671.

108. Pauwels E, Cleeren F, Tshibangu T, et al. [18F]AlF-NOTA-octreotide PET imaging: biodistribution, dosimetry and first comparison with [68Ga]Ga-DOTATATE in neuroendocrine tumour patients. *European Journal of Nuclear Medicine and Molecular Imaging.* 2020.

109. Long T, Yang N, Zhou M, et al. Clinical Application of 18F-AlF-NOTA-Octreotide PET/CT in Combination With 18F-FDG PET/CT for Imaging Neuroendocrine Neoplasms. *Clinical Nuclear Medicine.* 2019;44:452-458.

110. Sprague DR, Chin FT, Liow J-S, et al. Human biodistribution and radiation dosimetry of the tachykinin NK1 antagonist radioligand [^{18}F]SPA-RQ: comparison of thin -slice, bisected, and 2-D planar image analysis. *Journal of Nuclear Medicine.* 2007;48:100-107.

111. Bullich S, Barret O, Constantinescu C, et al. Evaluation of dosimetry, quantitative methods and test-retest variability of 18F-PI-2620 PET for the assessment of tau deposits in the human brain. *Journal of Nuclear Medicine.* 2019.

112. Choi JY, Lyoo CH, Lee JH, et al. Human Radiation Dosimetry of [(18)F]AV-1451(T807) to Detect Tau Pathology. *Mol Imaging Biol.* 2016;18:479-482.

113. Sanabria Bohorquez S, Marik J, Ogasawara A, et al. [(18)F]GTP1 (Genentech Tau Probe 1), a radioligand for detecting neurofibrillary tangle tau pathology in Alzheimer's disease. *Eur J Nucl Med Mol Imaging.* 2019;46:2077-2089.

114. Koole M, Lohith TG, Valentine JL, et al. Preclinical Safety Evaluation and Human Dosimetry of [(18)F]MK-6240, a Novel PET Tracer for Imaging Neurofibrillary Tangles. *Mol Imaging Biol.* 2020;22:173-180.

115. Wong DF, Comley RA, Kuwabara H, et al. Characterization of 3 Novel Tau Radiopharmaceuticals, (11)C-RO-963, (11)C-RO-643, and (18)F-RO-948, in Healthy Controls and in Alzheimer Subjects. *J Nucl Med.* 2018;59:1869-1876.

116. Hsiao IT, Lin KJ, Huang KL, et al. Biodistribution and Radiation Dosimetry for the Tau Tracer (18)F-THK-5351 in Healthy Human Subjects. *J Nucl Med.* 2017;58:1498-1503.

117. Schmidt ME, Janssens L, Moechars D, et al. Clinical evaluation of [18F] JNJ-64326067, a novel candidate PET tracer for the detection of tau pathology in Alzheimer's disease. *European Journal of Nuclear Medicine and Molecular Imaging.* 2020.

118. Fujimura Y, Kimura Y, Simeon FG, et al. Biodistribution and radiation dosimetry in humans of a new PET ligand, (18)F-PBR06, to image translocator protein (18 kDa). *J Nucl Med.* 2010;51:145-149.

119. Mizrahi R, Rusjan PM, Vitcu I, et al. Whole Body Biodistribution and Radiation Dosimetry in Humans of a New PET Ligand, [(18)F]-FEPPA, to Image Translocator Protein (18 kDa). *Mol Imaging Biol.* 2012.

120. Boellaard R, Sparks R, Hoffman A, et al. Radiation dose of [18F]DPA714 PET studies. *Journal of Nuclear Medicine.* 2011;52:1453.

121. Hino-Shishikura A, Suzuki A, Minamimoto R, et al. Biodistribution and radiation dosimetry of [(1)(8)F]-5-fluorouracil. *Appl Radiat Isot.* 2013;75:11-17.

122. Vesselle H, Grierson J, Peterson LM, Muzi M, Mankoff DA, Krohn KA. 18F-Fluorothymidine radiation dosimetry in human PET imaging studies. *J Nucl Med.* 2003;44:1482-1488.

123. Nye JA, Schuster DM, Yu W, Camp VM, Goodman MM, Votaw JR. Biodistribution and radiation dosimetry of the synthetic nonmetabolized amino acid analogue anti-18F-FACBC in humans. *J Nucl Med.* 2007;48:1017-1020.

124. McParland BJ, Wall A, Johansson S, Sorensen J. The clinical safety, biodistribution and internal radiation dosimetry of [(1)(8)F]fluciclovine in healthy adult volunteers. *Eur J Nucl Med Mol Imaging.* 2013;40:1256-1264.

125. Pauleit D, Floeth F, Herzog H, et al. Whole-body distribution and dosimetry of O-(2-[18F]fluoroethyl)-L-tyrosine. *Eur J Nucl Med Mol Imaging.* 2003;30:519-524.

126. Kurdziel KA, Kalen JD, Hirsch JI, et al. Human dosimetry and preliminary tumor distribution of 18F-fluoropaclitaxel in healthy volunteers and newly diagnosed breast cancer patients using PET/CT. *J Nucl Med.* 2011;52:1339-1345.

127. Borner AR, Langen KJ, Herzog H, et al. Whole-body kinetics and dosimetry of cis-4-[(18)F]fluoro-L-proline. *Nucl Med Biol.* 2001;28:287-292.

128. Smolarz K, Krause BJ, Graner FP, et al. (S)-4-(3-18F-Fluoropropyl)-L-Glutamic Acid: An 18F-Labeled Tumor-Specific Probe for PET/CT Imaging--Dosimetry. *J Nucl Med.* 2013.

129. Dehdashti F, Laforest R, Gao F, et al. Assessment of progesterone receptors in breast carcinoma by PET with 21-18F-fluoro-16alpha,17alpha-[(R)-(1'-alpha-furylmethylidene)dioxy]-19-norpregn- 4-ene-3,20-dione. *J Nucl Med.* 2012;53:363-370.

130. Dehdashti F, Laforest R, Gao F, et al. Assessment of Cellular Proliferation in Tumors by PET Using 18F-ISO-1. *J Nucl Med.* 2013;54:350-357.

131. Asano Y, Inoue Y, Ikeda Y, et al. Phase I clinical study of NMK36: a new PET tracer with the synthetic amino acid analogue anti-[18F]FACBC. *Ann Nucl Med.* 2011;25:414-418.

132. Krebs S, Veach DR, Carter LM, et al. First-in-Human Trial of Dasatinib-Derivative Tracer for Tumor Kinase-Targeted Positron Emission Tomography. *J Nucl Med.* 2020.

133. Xu X, Zhu H, Liu F, et al. Dynamic PET/CT imaging of (18)F-(2S, 4R)4-fluoroglutamine in healthy volunteers and oncological patients. *Eur J Nucl Med Mol Imaging.* 2020.

134. Venneti S, Dunphy MP, Zhang H, et al. Glutamine-based PET imaging facilitates enhanced metabolic evaluation of gliomas in vivo. *Sci Transl Med.* 2015;7:274ra217.

135. Young CR, Adler S, Eary JF, et al. Biodistribution, Tumor Detection, and Radiation Dosimetry of (18)F-5-Fluoro-2'-Deoxycytidine with Tetrahydrouridine in Solid Tumors. *J Nucl Med.* 2019;60:492-496.

136. Chantepie S, Hovhannisyan N, Guillouet S, et al. (18)F-Fludarabine PET for Lymphoma Imaging: First-in-Humans Study on DLBCL and CLL Patients. *J Nucl Med.* 2018;59:1380-1385.

137. Challapalli A, Sharma R, Hallett WA, et al. Biodistribution and radiation dosimetry of deuterium-substituted 18F-fluoromethyl-[1, 2-2H4]choline in healthy volunteers. *J Nucl Med.* 2014;55:256-263.

138. de Jong J, Kowal K, Zitzmann-Kolbe S, et al. Radiation dosimetry and biodistribution of BAY86-9596 (O-([18F]fluoromethyl)-D-tyrosine). *Journal of Nuclear Medicine.* 2011;52:1455.

139. Caveliers V, Kersemans K, Lahoutte T, et al. Human biodistribution, dosimetry and initial clinical results of 2-18F-fluoromethyl-L-phenylalanine, a new tumor tracer for PET. *Journal of Nuclear Medicine.* 2008;49:282P.

140. Krause BJ, Smolarz K, Graner F-P, et al. [18F]BAY 85-8050 (TIM-1): A novel tumor specific probe for PET/CT imaging - Dosimetry. *Journal of Nuclear Medicine.* 2010;51:1434.

141. Giesel F, Adeberg S, Syed M, et al. FAPI-74 PET/CT Using Either 18F-AlF or Cold-kit 68Ga-labeling: Biodistribution, Radiation Dosimetry and Tumor Delineation in Lung Cancer Patients. *Journal of Nuclear Medicine.* 2020.

142. Laforest R, Lui H, HUssain J, Cummings K, Perlmutter J, Tu Z. Radiation Dosimetry on 18F-VAT in human. *Journal of Nuclear Medicine.* 2018;59:1002.

143. Petrou M, Frey KA, Kilbourn MR, et al. In vivo imaging of human cholinergic nerve terminals with (-)-5-(18)F-fluoroethoxybenzovesamicol: biodistribution, dosimetry, and tracer kinetic analyses. *J Nucl Med.* 2014;55:396-404.

144. Lin KJ, Weng YH, Wey SP, et al. Whole-body biodistribution and radiation dosimetry of 18F-FP-(+)-DTBZ (18F-AV-133): a novel vesicular monoamine transporter 2 imaging agent. *J Nucl Med.* 2010;51:1480-1485.

Table 3: Tracers for which the human dosimetry has been estimated more than once. When the target organ is the same in both studies, their doses and their relative differences are reported.

	Effective dose (µSv/MBq)	Relative difference (%)	Target organ	Dose to the target organ (µSv/MBq)	Relative difference (%)	References
^{11}C Tracer						
ITMM [a]	4.4	4.6	Bladder	12.5	5.6	(*1*)
	4.6		Bladder	13.2		(*2*)
Pib	4.7	12.8	Gallbladder	41.5	8	(*3*)
	5.3		Gallbladder	44.8		(*4*)
Raclopride	6.3	6.3	Gallbladder			(*5*)
	6.7		Kidney			(*6*)
Flumazenil	5.2	46.2	Bladder	36.8	71.7	(*7*)
	7.6		Bladder	63.2		(*8*)
PK11195	5.1	N/A [b]	Kidney			(*9*)
	4.6 [b]		Bladder			(*10*)
Acetate	4.9	40	Pancreas			(*11*)
	3.5		Kidney			(*12*)
^{18}F Tracer						
BAY94-9172 (Florbetaben)	14.7	12.2	Gallbladder	132.4	28.5	(*4*)
	16.5		Gallbladder	103		(*13*)
AV-45 (florbetapir)	16	48.5 [c]	Gallbladder	150	539 [c]	(*14*)
	13		N/A	N/A		(*15*)
	19.3		Gallbladder	184.7		(*16*)
	18.6		Gallbladder	143		(*17*)
	17.8		Gallbladder	28.9		(*18*)
Flutemetamol (GE067)	33.8	30	Gallbladder			(*19*)
	26		Bladder			(*20*)
FBPA	23.9	59.3	Kidney			(*21*)
	15		Heart			(*22*)
FAC [a]	5.24	161.5	Bladder	20.4	173	(*23*)
	13.7		Bladder	55.7		(*24*)
16α-F-estradiol	27	N/A [b]	Gallbladder			(*25*)
	22 [b]		Liver			(*26*)
BAY 864367	23	60.8	Gallbladder			(*27*)
	14.3		Bladder			(*28*)
FDG	29	93.3 [c]	Bladder	94.2	496.2 [c]	(*29*)
	24 [d]		Bladder	310		(*30*)
	15		Bladder	73		(*31*)
	15.3		Bladder	52		(*32*)
	19.9		Bladder	84.6		(*33*)
EF5	18	27.8	Bladder	120	41.7	(*34*)
	23		Bladder	170		(*35*)
FPEB	25	47.9	Bladder			(*36*)
	16.9		Gallbladder			(*37*)

A-85380	19.4	101 [c]	Bladder	81.8	120 [c]	(*38*)
	39		Bladder	180		(*39*)
	23.7		Bladder	153		(*40*)
F-choline	18 [e]	N/A [b]	Kidney	79	115.2	(*41*)
	34.1 [b]		Kidney	170		(*42*)
AIF-OC	22.4	3.1	Spleen	159	12	(*43*)
	23.1		Spleen	142		(*44*)
FDHT	12.5 [f]	60	Bladder	86.8	42.3	(*45*)
	20		Bladder	61		(*46*)
DCFPyL [a]	17	22.3	Lacrimal glands			(*47*)
	13.9		Kidney			(*48*)
Tetrafluoroborate	50	53.4	Thyroid	31	335.5	(*49*)
	32.6		Thyroid	135		(*50*)
FACBC (GE-148) (fluciclovine)	14.1	56.7	Liver			(*51*)
	22.1		Pancreas			(*52*)
(2S, 4R)4-fluoroglutamine	19.4	2.6	Uterus			(*53*)
	18.9		Bladder			(*54*)

Relative differences are the ratio of the difference between the two values over the smaller value.

If one of the values is expressed as Effective Dose Equivalent, the difference is not calculated.

[a] Tracer for which both dosimetry studies were performed by the same team

[b] Effective Dose Equivalent

[c] Difference between the highest and lowest value

[d] Effective dose is estimated to be higher than total-body dose by approximately a factor of two

[e] Risk-weighted absorbed dose coefficient

[f] Value estimated from the data reported in the original paper (estimations taken from (*55*))

References

1. Ito K, Sakata M, Oda K, et al. Comparison of dosimetry between PET/CT and PET alone using (11)C-ITMM. *Australas Phys Eng Sci Med.* 2016;39:177-186.

2. Toyohara J, Sakata M, Oda K, et al. Initial human PET studies of metabotropic glutamate receptor type 1 ligand 11C-ITMM. *J Nucl Med.* 2013;54:1302-1307.

3. Scheinin NM, Tolvanen TK, Wilson IA, Arponen EM, Nagren KA, Rinne JO. Biodistribution and radiation dosimetry of the amyloid imaging agent 11C-PIB in humans. *J Nucl Med.* 2007;48:128-133.

4. O'Keefe GJ, Saunder TH, Ng S, et al. Radiation dosimetry of beta-amyloid tracers 11C-PiB and 18F-BAY94-9172. *J Nucl Med.* 2009;50:309-315.

5. Slifstein M, Hwang DR, Martinez D, et al. Biodistribution and radiation dosimetry of the dopamine D2 ligand 11C-raclopride determined from human whole-body PET. *J Nucl Med.* 2006;47:313-319.

6. Ribeiro MJ, Ricard M, Bourgeois S, et al. Biodistribution and radiation dosimetry of [11C]raclopride in healthy volunteers. *Eur J Nucl Med Mol Imaging.* 2005;32:952-958.

7. Nugent AC, Neumeister A, Drevets WC, Eckelman WC, Channing MA, Herscovitch P. Human biodistribution and dosimetry of the PET benzodiazepine receptor ligand 11C-flumazenil. *Journal of Nuclear Medicine.* 2004;45(suppl):434P.

8. Laymon CM, Narendran R, Mason NS, et al. Human biodistribution and dosimetry of the PET radioligand [(1)(1)C]flumazenil (FMZ). *Mol Imaging Biol.* 2012;14:115-122.

9. Hirvonen J, Roivainen A, Virta J, Helin S, Nagren K, Rinne JO. Human biodistribution and radiation dosimetry of 11C-(R)-PK11195, the prototypic PET ligand to image inflammation. *Eur J Nucl Med Mol Imaging.* 2010;37:606-612.

10. Kumar A, Muzik O, Chugani D, Chakraborty P, Chugani HT. PET-derived biodistribution and dosimetry of the benzodiazepine receptor-binding radioligand (11)C-(R)-PK11195 in children and adults. *J Nucl Med.* 2010;51:139-144.

11. Seltzer MA, Jahan SA, Sparks R, et al. Radiation dose estimates in humans for (11)C-acetate whole-body PET. *J Nucl Med.* 2004;45:1233-1236.

12. Liu D, Khong PL, Gao Y, et al. Radiation Dosimetry of Whole-Body Dual-Tracer 18F-FDG and 11C-Acetate PET/CT for Hepatocellular Carcinoma. *J Nucl Med.* 2016;57:907-912.

13. Sattler B, Seese A, Barthel H, et al. Radiation risk caused by [F18]BAY 94-9172, a new PET tracer for detection of cerebral β-amyloid plaques. *Journal of Nuclear Medicine.* 2009;50:1840.

14. Adler L, Wolodzko J, Stabin M, McNelis T, Gammage L, Joshi A. Radiation dosimetry of F18-AV-45 measured by PET/CT in humans. *Journal of Nuclear Medicine.* 2008;49 (Suppl 1:283).

15. Wong DF, Rosenberg PB, Zhou Y, et al. In vivo imaging of amyloid deposition in Alzheimer disease using the radioligand 18F-AV-45 (florbetapir [corrected] F 18). *J Nucl Med.* 2010;51:913-920.

16. Lin KJ, Hsu WC, Hsiao IT, et al. Whole-body biodistribution and brain PET imaging with [18F]AV-45, a novel amyloid imaging agent--a pilot study. *Nucl Med Biol.* 2010;37:497-508.

17. Joshi AD, Pontecorvo MJ, Adler L, et al. Radiation dosimetry of florbetapir F 18. *EJNMMI Res.* 2014;4:4.

18. Nakano M, Nakamura T, Takita Y, et al. Radiation dosimetry and pharmacokinetics of florbetapir ((18)F) in Japanese subjects. *Ann Nucl Med.* 2019;33:639-645.

19. Koole M, Lewis DM, Buckley C, et al. Whole-body biodistribution and radiation dosimetry of 18F-GE067: a radioligand for in vivo brain amyloid imaging. *J Nucl Med.* 2009;50:818-822.

20. Senda M, Sasaki M, Fujikawa K, Paterson C, McParland B. Biodistribution and radiation dosimetry of Flutemetamol (18F) injection in Japanese healthy volunteers. *Journal of Nuclear Medicine.* 2012;53:1510.

21. Sakata M, Oda K, Toyohara J, Ishii K, Nariai T, Ishiwata K. Direct comparison of radiation dosimetry of six PET tracers using human whole-body imaging and murine biodistribution studies. *Ann Nucl Med.* 2013;27:285-296.

22. Kono Y, Kurihara H, Kawamoto H, et al. Radiation absorbed dose estimates for 18F-BPA PET. *Acta Radiol.* 2017;58:1094-1100.

23. Schwarzenberg J, Radu CG, Benz M, et al. Human biodistribution and radiation dosimetry of novel PET probes targeting the deoxyribonucleoside salvage pathway. *Eur J Nucl Med Mol Imaging.* 2011;38:711-721.

24. Benz M, Radu C, Allen-Auerbach M, et al. Human biodistribution and dosimetry of the nucleoside analogue [18F]FAC in humans. *Journal of Nuclear Medicine.* 2008;49:284P.

25. Beauregard JM, Croteau E, Ahmed N, van Lier JE, Benard F. Assessment of human biodistribution and dosimetry of 4-fluoro-11beta-methoxy-16alpha-18F-fluoroestradiol using serial whole-body PET/CT. *J Nucl Med.* 2009;50:100-107.

26. Mankoff DA, Peterson LM, Tewson TJ, et al. [18F]fluoroestradiol radiation dosimetry in human PET studies. *J Nucl Med.* 2001;42:679-684.

27. Smolarz K, Krause BJ, Schmelz Y, et al. Human biodistribution and radiation dosimetry of BAY 86-4367: A F-18 labeled bombesin antagonist for PET/CT imaging of prostate cancer. *Journal of Nuclear Medicine.* 2011;52:1456.

28. Sah BR, Burger IA, Schibli R, et al. Dosimetry and first clinical evaluation of the new 18F-radiolabeled bombesin analogue BAY 864367 in patients with prostate cancer. *J Nucl Med.* 2015;56:372-378.

29. Deloar HM, Fujiwara T, Shidahara M, et al. Estimation of absorbed dose for 2-[F-18]fluoro-2-deoxy-D-glucose using whole-body positron emission tomography and magnetic resonance imaging. *Eur J Nucl Med.* 1998;25:565-574.

30. Hays MT, Watson EE, Thomas SR, Stabin M. MIRD dose estimate report no. 19: radiation absorbed dose estimates from (18)F-FDG. *J Nucl Med.* 2002;43:210-214.

31. Staaf J, Jacobsson H, Sanchez-Crespo A. A revision of the organ radiation doses from 2-fluoro-2-deoxy-D-glucose with reference to tumour presence. *Radiat Prot Dosimetry.* 2012;151:43-50.

32. Srinivasan S, Crandall JP, Gajwani P, et al. Human Radiation Dosimetry for Orally and Intravenously Administered 18F-FDG. *Journal of Nuclear Medicine.* 2020;61:613-619.

33. Quinn B, Dauer Z, Pandit-Taskar N, Schoder H, Dauer LT. Radiation dosimetry of 18F-FDG PET/CT: incorporating exam-specific parameters in dose estimates. *BMC Med Imaging.* 2016;16:41.

34. Lin LL, Silvoniemi A, Stubbs JB, et al. Radiation dosimetry and biodistribution of the hypoxia tracer (18)F-EF5 in oncologic patients. *Cancer Biother Radiopharm.* 2012;27:412-419.

35. Koch CJ, Scheuermann JS, Divgi C, et al. Biodistribution and dosimetry of (18)F-EF5 in cancer patients with preliminary comparison of (18)F-EF5 uptake versus EF5 binding in human glioblastoma. *Eur J Nucl Med Mol Imaging.* 2010;37:2048-2059.

36. Kessler RM, Seibyl J, Cowan RL, et al. Radiation Dosimetry of (18)F-FPEB in Humans. *J Nucl Med.* 2014;55:1119-1121.

37. Wong DF, Waterhouse R, Kuwabara H, et al. 18F-FPEB, a PET radiopharmaceutical for quantifying metabotropic glutamate 5 receptors: a first-in-human study of radiochemical safety, biokinetics, and radiation dosimetry. *J Nucl Med.* 2013;54:388-396.

38. Bottlaender M, Valette H, Roumenov D, et al. Biodistribution and radiation dosimetry of 18F-fluoro-A-85380 in healthy volunteers. *J Nucl Med.* 2003;44:596-601.

39. Kimes AS, Horti AG, London ED, et al. 2-[^{18}F]F-A-85380: PET imaging of brain nicotinic acetylcholine receptors and whole body distribution in humans. *FASEB J.* 2003;17:1331-1333.

40. Obrzut SL, Koren AO, Mandelkern MA, Brody AL, Hoh CK, London ED. Whole-body radiation dosimetry of 2-[18F]Fluoro-A-85380 in human PET imaging studies. *Nucl Med Biol.* 2005;32:869-874.

41. Giussani A, Janzen T, Uusijarvi-Lizana H, et al. A compartmental model for biokinetics and dosimetry of 18F-choline in prostate cancer patients. *J Nucl Med.* 2012;53:985-993.

42. DeGrado TR, Reiman RE, Price DT, Wang S, Coleman RE. Pharmacokinetics and radiation dosimetry of 18F-fluorocholine. *J Nucl Med.* 2002;43:92-96.

43. Pauwels E, Cleeren F, Tshibangu T, et al. [18F]AlF-NOTA-octreotide PET imaging: biodistribution, dosimetry and first comparison with [68Ga]Ga-DOTATATE in neuroendocrine tumour patients. *European Journal of Nuclear Medicine and Molecular Imaging.* 2020.

44. Long T, Yang N, Zhou M, et al. Clinical Application of 18F-AlF-NOTA-Octreotide PET/CT in Combination With 18F-FDG PET/CT for Imaging Neuroendocrine Neoplasms. *Clinical Nuclear Medicine.* 2019;44:452-458.

45. Zanzonico PB, Finn R, Pentlow KS, et al. PET-based radiation dosimetry in man of 18F-fluorodihydrotestosterone, a new radiotracer for imaging prostate cancer. *J Nucl Med.* 2004;45:1966-1971.

46. McCall K, Abbott A, Hu J, et al. Report on the PET/CT image-based radiation dosimetry of 18FDHT in women, an imaging agent with new applications for evaluation of androgen receptor status in patients with metastatic breast cancer. *Journal of Nuclear Medicine.* 2019;60:1630.

47. Plyku D, Mena E, Rowe SP, et al. Combined model-based and patient-specific dosimetry for (18)F-DCFPyL, a PSMA-targeted PET agent. *Eur J Nucl Med Mol Imaging.* 2018;45:989-998.

48. Szabo Z, Mena E, Rowe SP, et al. Initial Evaluation of [(18)F]DCFPyL for Prostate-Specific Membrane Antigen (PSMA)-Targeted PET Imaging of Prostate Cancer. *Mol Imaging Biol.* 2015;17:565-574.

49. Jiang H, Schmit NR, Koenen AR, et al. Safety, pharmacokinetics, metabolism and radiation dosimetry of (18)F-tetrafluoroborate ((18)F-TFB) in healthy human subjects. *EJNMMI Res.* 2017;7:90.

50. O'Doherty J, Jauregui-Osoro M, Brothwood T, et al. (18)F-Tetrafluoroborate, a PET Probe for Imaging Sodium/Iodide Symporter Expression: Whole-Body Biodistribution, Safety, and Radiation Dosimetry in Thyroid Cancer Patients. *J Nucl Med.* 2017;58:1666-1671.

51. Nye JA, Schuster DM, Yu W, Camp VM, Goodman MM, Votaw JR. Biodistribution and radiation dosimetry of the synthetic nonmetabolized amino acid analogue anti-18F-FACBC in humans. *J Nucl Med.* 2007;48:1017-1020.

52. McParland BJ, Wall A, Johansson S, Sorensen J. The clinical safety, biodistribution and internal radiation dosimetry of [(1)(8)F]fluciclovine in healthy adult volunteers. *Eur J Nucl Med Mol Imaging.* 2013;40:1256-1264.

53. Xu X, Zhu H, Liu F, et al. Dynamic PET/CT imaging of (18)F-(2S, 4R)4-fluoroglutamine in healthy volunteers and oncological patients. *Eur J Nucl Med Mol Imaging.* 2020.

54. Venneti S, Dunphy MP, Zhang H, et al. Glutamine-based PET imaging facilitates enhanced metabolic evaluation of gliomas in vivo. *Sci Transl Med.* 2015;7:274ra217.

55. Kimura Y, Simeon FG, Hatazawa J, et al. Biodistribution and radiation dosimetry of a positron emission tomographic ligand, 18F-SP203, to image metabotropic glutamate subtype 5 receptors in humans. *Eur J Nucl Med Mol Imaging.* 2010;37:1943-1949.

Table 4: Effective dose extrapolated from monkeys and measured directly in humans, and their relative difference.

	Effective dose from monkeys (µSv/MBq)	Effective dose from humans (µSv/MBq)	% difference compared to the human dose	References
^{11}C Tracer				
Rolipram	6.6	4.8	38	(*1*)
DASB	6	7	-14	(*2,3*)
PBR28	10.3	6.6	56	(*4*)
CUMI-101	6.9	5.3	30	(*5*); Parsey unpubl
MePPEP	6.6	4.6	43	(*6*); NIMH data
dLop	9.4	7.8	21	(*7,8*)
PK11195	5.3	5.1	4	(*9,10*); NIMH data
		4.6 [a]	N/A	
Raclopride	6.7	6.3	6	(*11-13*)
		6.7	0	
GSK931145	5.2	4.5	16	(*14*)
NNC112	3.9	5.7	-32	(*15,16*)
Erlotinib	3.7	3.6	3	(*17*)
MK-8278	4.8	5.4	11	(*18*)
PHNO	5	4.5	11	(*19,20*)
Pib	7.4	4.7	57	(*21-23*)
		5.3	40	
NOP1	5	4.3	16	(*24,25*)
UCB-J	3.3	7.6	-57	(*26,27*)
^{18}F Tracer				
FMPEP-d2	25.1	19.7	27	(*6*); NIMH data
RGD-K5	40	31	29	(*28*)
FPEB	23.7	16.9	98 [b]	(*29-32*)
	33.5	25		
SP203	27	17.8	52	(*33*); NIMH data

BMS747158	15	19	-21	(*34,35*)
PBR06	30.3	18.5	64	(*36*); NIMH data
Fluoropaclitaxel	22	28.8	-24	(*37,38*)
PF-06684511	43	24.7	74	(*39,40*)
AV1451 (T807)	18.9	22.5	-16	(*41,42*)
Fluortriopride	20 [c]	22.5	-11	(*43,44*)
FE-PE2I	21	23	-9	(*45,46*)
Tetrafluoroborate	24.7	50	-51	(*47-49*)
		32.6	-24	
PF-05270430	21.7	34.9	-38	(*50,51*)
	24.9		-29	
VAT	17.5	12	46	(*52,53*)
FIMX	25.4	23.4	9	(*54*); NIMH data
MNI-444	21.9 [d]	23.1	-5	(*55,56*)
LMI1195	18.9	26	-27	(*57,58*)
MNI-659	19.7	24.1	-18	(*31,59*)
HX4	42	27	56	(*60*)
FMeNER-D2	33.2	17	95	(*61,62*)
LSN3316612	22	20.5	7	(*63,64*)

[a] Effective dose equivalent (*10*). By consequence, the comparison with the ED from monkeys is not calculated.

[b] Largest difference between the two monkey studies (*31,32*) and the two human studies (*29,30*).

[c] Different values of effective dose extrapolated from monkeys are given (*44*). We chose the one that is the closest to the human dose (*43*).

[d] Two different ED values were estimated with two different approaches. We report here the one (Scaled Monkey Organ Weight) that gives the closest approximation to human data (+5%). The other approach (No Correction for Organ Weight Difference) would have given a difference of -23% (*55*).

References

1. Sprague DR, Fujita M, Ryu YH, Liow JS, Pike VW, Innis RB. Whole-body biodistribution and radiation dosimetry in monkeys and humans of the phosphodiesterase 4 radioligand [(11)C](R)-rolipram: comparison of two-dimensional planar, bisected and quadrisected image analyses. *Nucl Med Biol.* 2008;35:493-500.

2. Lu JQ, Ichise M, Liow JS, Ghose S, Vines D, Innis RB. Biodistribution and radiation dosimetry of the serotonin transporter ligand 11C-DASB determined from human whole-body PET. *J Nucl Med.* 2004;45:1555-1559.

3. Tipre DN, Lu J-Q, Fujita M, Ichise M, Vines D, Innis RB. Radiation dosimetry estimates for the PET serotonin transporter probe [^{11}C]DASB determined from whole-body imaging in nonhuman primates. *Nucl Med Comm.* 2004;25:81-86.

4. Brown AK, Fujita M, Fujimura Y, et al. Radiation dosimetry and biodistribution in monkey and man of 11C-PBR28: a PET radioligand to image inflammation. *J Nucl Med.* 2007;48:2072-2079.

5. Hines CS, Liow J-S, Zanotti-Fregonara P, et al. Human biodistribution and dosimetry of 11C-CUMI-101, an agonist radioligand for serotonin-1A receptors in brain. *PloS one.* 2011;6:e25309.

6. Terry GE, Hirvonen J, Liow JS, et al. Biodistribution and dosimetry in humans of two inverse agonists to image cannabinoid CB1 receptors using positron emission tomography. *Eur J Nucl Med Mol Imaging.* 2010;37:1499-1506.

7. Liow JS, Kreisl W, Zoghbi SS, et al. P-glycoprotein function at the blood-brain barrier imaged using 11C-N-desmethyl-loperamide in monkeys. *J Nucl Med.* 2009;50:108-115.

8. Seneca N, Zoghbi SS, Liow JS, et al. Human brain imaging and radiation dosimetry of 11C-N-desmethyl-loperamide, a PET radiotracer to measure the function of P-glycoprotein. *J Nucl Med.* 2009;50:807-813.

9. Hirvonen J, Roivainen A, Virta J, Helin S, Nagren K, Rinne JO. Human biodistribution and radiation dosimetry of 11C-(R)-PK11195, the prototypic PET ligand to image inflammation. *Eur J Nucl Med Mol Imaging.* 2010;37:606-612.

10. Kumar A, Muzik O, Chugani D, Chakraborty P, Chugani HT. PET-derived biodistribution and dosimetry of the benzodiazepine receptor-binding radioligand (11)C-(R)-PK11195 in children and adults. *J Nucl Med.* 2010;51:139-144.

11. Ribeiro MJ, Ricard M, Bourgeois S, et al. Biodistribution and radiation dosimetry of [11C]raclopride in healthy volunteers. *Eur J Nucl Med Mol Imaging.* 2005;32:952-958.

12. Slifstein M, Hwang DR, Martinez D, et al. Biodistribution and radiation dosimetry of the dopamine D2 ligand 11C-raclopride determined from human whole-body PET. *J Nucl Med.* 2006;47:313-319.

13. Herscovitch P, Schmall B, Doudet DJ, Carson RE, Eckelman WC. Biodistribution and radiation dose estimates for [C-11]raclopride. *Journal of Nuclear Medicine.* 1997;38:951-951.

14. Bullich S, Slifstein M, Passchier J, et al. Biodistribution and radiation dosimetry of the glycine transporter-1 ligand 11C-GSK931145 determined from primate and human whole-body PET. *Mol Imaging Biol.* 2011;13:776-784.

15. Cropley VL, Fujita M, Musachio JL, et al. Whole-body biodistribution and estimation of radiation-absorbed doses of the dopamine D1 receptor radioligand 11C-NNC 112 in humans. *J Nucl Med.* 2006;47:100-104.

16. Moerlein S, Laforest R, Antenor J, Permutter J. Absorbed radiation dosimetry of the D1 ligand 11C-NNC 112 as determined by whole-body PET imaging of baboons. *Journal of Nuclear Medicine.* 2006;47:494P.

17. Petrulli JR, Hansen SB, Abourbeh G, et al. A multi species evaluation of the radiation dosimetry of [(11)C]erlotinib, the radiolabeled analog of a clinically utilized tyrosine kinase inhibitor. *Nucl Med Biol.* 2017;47:56-61.

18. Van Laere KJ, Sanabria-Bohorquez SM, Mozley DP, et al. (11)C-MK-8278 PET as a tool for pharmacodynamic brain occupancy of histamine 3 receptor inverse agonists. *J Nucl Med.* 2014;55:65-72.

19. Gallezot J-D, Beaver J, Nabulsi N, et al. [11C]PHNO studies in rhesus monkey: In vivo affinity for D2 and D3 receptors and dosimetry. *Journal of Nuclear Medicine.* 2009;50:601.

20. Mizrahi R, Rusjan P, Vitcu I, et al. Whole-body distribution and radiation dosimetry of 11C-(+)-PHNO, a D2/3 agonist ligand. *J Nucl Med.* 2012;53:1802-1806.

21. Parsey RV, Sokol LO, Belanger MJ, et al. Amyloid plaque imaging agent [C-11]-6-OH-BTA-1: biodistribution and radiation dosimetry in baboon. *Nucl Med Commun.* 2005;26:875-880.

22. O'Keefe GJ, Saunder TH, Ng S, et al. Radiation dosimetry of beta-amyloid tracers 11C-PiB and 18F-BAY94-9172. *J Nucl Med.* 2009;50:309-315.

23. Scheinin NM, Tolvanen TK, Wilson IA, Arponen EM, Nagren KA, Rinne JO. Biodistribution and radiation dosimetry of the amyloid imaging agent 11C-PIB in humans. *J Nucl Med.* 2007;48:128-133.

24. Lohith TG, Zoghbi SS, Morse CL, et al. Brain and whole-body imaging of nociceptin/orphanin FQ peptide receptor in humans using the PET ligand 11C-NOP-1A. *J Nucl Med.* 2012;53:385-392.

25. Kimura Y, Fujita M, Hong J, et al. Brain and whole-body imaging in rhesus monkeys of 11C-NOP-1A, a promising PET radioligand for nociceptin/orphanin FQ peptide receptors. *J Nucl Med.* 2011;52:1638-1645.

26. Bini J, Holden D, Fontaine K, et al. Human adult and adolescent biodistribution and dosimetry of the synaptic vesicle glycoprotein 2A radioligand 11C-UCB-J. *EJNMMI Research.* 2020;10:83.

27. Nabulsi NB, Mercier J, Holden D, et al. Synthesis and Preclinical Evaluation of 11C-UCB-J as a PET Tracer for Imaging the Synaptic Vesicle Glycoprotein 2A in the Brain. *J Nucl Med.* 2016;57:777-784.

28. Doss M, Kolb HC, Zhang JJ, et al. Biodistribution and radiation dosimetry of the integrin marker 18F-RGD-K5 determined from whole-body PET/CT in monkeys and humans. *J Nucl Med.* 2012;53:787-795.

29. Kessler RM, Seibyl J, Cowan RL, et al. Radiation Dosimetry of (18)F-FPEB in Humans. *J Nucl Med.* 2014;55:1119-1121.

30. Wong DF, Waterhouse R, Kuwabara H, et al. 18F-FPEB, a PET radiopharmaceutical for quantifying metabotropic glutamate 5 receptors: a first-in-human study of radiochemical safety, biokinetics, and radiation dosimetry. *J Nucl Med.* 2013;54:388-396.

31. Constantinescu C, Barret O, Tavares A, et al. A comparative study between whole-body dosimetry estimates of [18F]FPEB, [18F]MNI-659, and [18F]MNI-444 in non-human primates and humans. *Journal of Nuclear Medicine.* 2015;56:1016.

32. Bélanger MJ, Krause SM, Ryan C, et al. Biodistribution and radiation dosimetry of [18F]F-PEB in nonhuman primates. *Nucl Med Commun.* 2008;29:915-919.

33. Kimura Y, Simeon FG, Hatazawa J, et al. Biodistribution and radiation dosimetry of a positron emission tomographic ligand, 18F-SP203, to image metabotropic glutamate subtype 5 receptors in humans. *Eur J Nucl Med Mol Imaging.* 2010;37:1943-1949.

34. Maddahi J, Czernin J, Lazewatsky J, et al. Phase I, first-in-human study of BMS747158, a novel 18F-labeled tracer for myocardial perfusion PET: dosimetry, biodistribution, safety, and imaging characteristics after a single injection at rest. *J Nucl Med.* 2011;52:1490-1498.

35. Lazewatsky J, Azure M, Guaraldi M, et al. Dosimetry of BMS747158, a novel 18F labeled tracer for myocardial perfusion imaging, in nonhuman primates at rest. *Journal of Nuclear Medicine.* 2008;49:15P.

36. Fujimura Y, Kimura Y, Simeon FG, et al. Biodistribution and radiation dosimetry in humans of a new PET ligand, (18)F-PBR06, to image translocator protein (18 kDa). *J Nucl Med.* 2010;51:145-149.

37. Kurdziel KA, Kalen JD, Hirsch JI, et al. Human dosimetry and preliminary tumor distribution of 18F-fluoropaclitaxel in healthy volunteers and newly diagnosed breast cancer patients using PET/CT. *J Nucl Med.* 2011;52:1339-1345.

38. Kurdziel KA, Kiesewetter DO, Carson RE, Eckelman WC, Herscovitch P. Biodistribution, Radiation Dose Estimates, and In Vivo Pgp Modulation Studies of 18F-Paclitaxel in Nonhuman Primates. *Journal of Nuclear Medicine.* 2003;44:1330-1339.

39. Arakawa R, Takano A, Stenkrona P, et al. PET imaging of beta-secretase 1 in the human brain: radiation dosimetry, quantification, and test-retest examination of [18F]PF-06684511. *European Journal of Nuclear Medicine and Molecular Imaging.* 2020.

40. Takano A, Chen L, Nag S, et al. Quantitative Analysis of 18F-PF-06684511, a Novel PET Radioligand for Selective β-Secretase 1 Imaging, in Nonhuman Primate Brain. *Journal of Nuclear Medicine.* 2019;60:992-997.

41. Choi JY, Lyoo CH, Lee JH, et al. Human Radiation Dosimetry of [(18)F]AV-1451(T807) to Detect Tau Pathology. *Mol Imaging Biol.* 2016;18:479-482.

42. Huang YY, Chiu MJ, Yen RF, et al. An one-pot two-step automated synthesis of [18F]T807 injection, its biodistribution in mice and monkeys, and a preliminary study in humans. *PLoS One.* 2019;14:e0217384.

43. Doot RK, Dubroff JG, Scheuermann JS, et al. Validation of gallbladder absorbed radiation dose reduction simulation: human dosimetry of [(18)F]fluortriopride. *EJNMMI Phys.* 2018;5:21.

44. Laforest R, Karimi M, Moerlein SM, et al. Absorbed radiation dosimetry of the D3-specific PET radioligand [(18)F]FluorTriopride estimated using rodent and nonhuman primate. *Am J Nucl Med Mol Imaging.* 2016;6:301-309.

45. Lizana H, Johansson L, Axelsson J, et al. Whole-Body Biodistribution and Dosimetry of the Dopamine Transporter Radioligand (18)F-FE-PE2I in Human Subjects. *J Nucl Med.* 2018;59:1275-1280.

46. Varrone A, Gulyas B, Takano A, Stabin MG, Jonsson C, Halldin C. Simplified quantification and whole-body distribution of [18F]FE-PE2I in nonhuman primates: prediction for human studies. *Nucl Med Biol.* 2012;39:295-303.

47. Jiang H, Schmit NR, Koenen AR, et al. Safety, pharmacokinetics, metabolism and radiation dosimetry of (18)F-tetrafluoroborate ((18)F-TFB) in healthy human subjects. *EJNMMI Res.* 2017;7:90.

48. Marti-Climent JM, Collantes M, Jauregui-Osoro M, et al. Radiation dosimetry and biodistribution in non-human primates of the sodium/iodide PET ligand [(18)F]-tetrafluoroborate. *EJNMMI Res.* 2015;5:70.

49. O'Doherty J, Jauregui-Osoro M, Brothwood T, et al. (18)F-Tetrafluoroborate, a PET Probe for Imaging Sodium/Iodide Symporter Expression: Whole-Body Biodistribution, Safety, and Radiation Dosimetry in Thyroid Cancer Patients. *J Nucl Med.* 2017;58:1666-1671.

50. Constantinescu C, Cole P, Brown T, et al. Radiation dosimetry and biodistribution of [18F]PF-05270430, a radiotracer for phosphodiesterase 2A (PDE2A) in rhesus macaques and humans. *Journal of Nuclear Medicine.* 2018;59:1012.

51. Naganawa M, Waterhouse RN, Nabulsi N, et al. First-in-Human Assessment of the Novel PDE2A PET Radiotracer 18F-PF-05270430. *J Nucl Med.* 2016;57:1388-1395.

52. Karimi M, Tu Z, Yue X, et al. Radiation dosimetry of [(18)F]VAT in nonhuman primates. *EJNMMI Res.* 2015;5:73.

53. Laforest R, Lui H, HUssain J, Cummings K, Perlmutter J, Tu Z. Radiation Dosimetry on 18F-VAT in human. *Journal of Nuclear Medicine.* 2018;59:1002.

54. Zanotti-Fregonara P, Xu R, Zoghbi SS, et al. The PET Radioligand 18F-FIMX Images and Quantifies Metabotropic Glutamate Receptor 1 in Proportion to the Regional Density of Its Gene Transcript in Human Brain. *J Nucl Med.* 2016;57:242-247.

55. Barret O, Hannestad J, Alagille D, et al. Adenosine 2A Receptor Occupancy by Tozadenant and Preladenant in Rhesus Monkeys. *Journal of Nuclear Medicine.* 2014;55:1712-1718.

56. Barret O, Hannestad J, Vala C, et al. Characterization in humans of 18F-MNI-444, a PET radiotracer for brain adenosine 2A receptors. *J Nucl Med.* 2015;56:586-591.

57. Mistry M, Kagan M, Lazewatsky J, et al. Dosimetry in nonhuman primates of [18F]LMI1195, a novel PET tracer for imaging the cardiac sympathetic nervous system. *Journal of Nuclear Medicine.* 2010;51:1447.

58. Sinusas AJ, Lazewatsky J, Brunetti J, et al. Biodistribution and radiation dosimetry of LMI1195: first-in-human study of a novel 18F-labeled tracer for imaging myocardial innervation. *J Nucl Med.* 2014;55:1445-1451.

59. Barret O, Thomae D, Tavares A, et al. In vivo assessment and dosimetry of 2 novel PDE10A PET radiotracers in humans: 18F-MNI-659 and 18F-MNI-654. *J Nucl Med.* 2014;55:1297-1304.

60. Doss M, Zhang JJ, Belanger MJ, et al. Biodistribution and radiation dosimetry of the hypoxia marker 18F-HX4 in monkeys and humans determined by using whole-body PET/CT. *Nucl Med Commun.* 2010;31:1016-1024.

61. Seneca N, Andree B, Sjoholm N, et al. Whole-body biodistribution, radiation dosimetry estimates for the PET norepinephrine transporter probe (S,S)-[18F]FMeNER-D2 in non-human primates. *Nucl Med Commun.* 2005;26:695-700.

62. Takano A, Halldin C, Varrone A, et al. Biodistribution and radiation dosimetry of the norepinephrine transporter radioligand (S,S)-[18F]FMeNER-D2: a human whole-body PET study. *Eur J Nucl Med Mol Imaging.* 2008;35:630-636.

63. Lee JH, Liow JS, Paul S, et al. PET quantification of brain O-GlcNAcase with [(18)F]LSN3316612 in healthy human volunteers. *EJNMMI Res.* 2020;10:20.

64. Paul S, Haskali MB, Liow JS, et al. Evaluation of a PET Radioligand to Image O-GlcNAcase in Brain and Periphery of Rhesus Monkey and Knock-Out Mouse. *J Nucl Med.* 2019;60:129-134.

Table 5: Target organs in monkeys and humans for the same tracers. The doses and their differences are reported only for the 11 tracers for which monkey and human data identified the same target organ

	Target organ from monkeys	Dose from monkeys (μSv/MBq)	Target organ from humans	Dose from humans (μSv/MBq)	% difference in organ dose compared to the human dose	References
^{11}C Tracer						
Rolipram	Bladder		Gallbladder			(*1*)
DASB	Bladder		Lungs			(*2,3*)
PBR28	Lungs		Kidney			(*4*)
CUMI-101	Bladder		Pancreas			(*5*); Parsey unpubl
MePPEP	N/A		Liver			(*6*); NIMH data
dLop	Thyroid		Kidney			(*7,8*)
PK11195	N/A		Kidney			(*9,10*); NIMH data
			Bladder			
Raclopride	Gallbladder		Gallbladder			(*11-13*)
			Kidney			
GSK931145	Liver	18.1	Liver	11.5	57	(*14*)
NNC112	Kidney		Gallbladder			(*15,16*)
Erlotinib	Liver	17.4	Liver	29.4	-41	(*17*)
MK-8278	N/A		Pancreas			(*18*)
PHNO	Kidney		Liver			(*19,20*)
Pib	Gallbladder	41	Gallbladder	41.5	-1	(*21-23*)
			Gallbladder	44.8	-8	
NOP1	Gallbladder	35.6	Gallbladder	21	70	(*24,25*)
UCB-J	Liver(males) Brain (females)		Bladder (males) Liver (females)			(*26,27*)
^{18}F Tracer						
FMPEP-d2	Bladder	135	Bladder	66.2	104	(*6*); NIMH data
RGD-K5	Bladder	400	Bladder	376	6	(*28*)
FPEB	Gallbladder Upper intestine		Gallbladder Bladder			(*29-32*)

SP203	N/A		Bladder			(*33*); NIMH data
BMS747158	Heart		Kidney			(*34,35*)
PBR06	Gallbladder	199	Gallbladder	367	-46	(*36*); NIMH data
Fluoropaclitaxel	Gallbladder	190	Gallbladder	229.5	-17	(*37,38*)
PF-06684511	N/A		Pancreas			(*39,40*)
AV1451 (T807)	Kidney		Liver			(*41,42*)
Fluortriopride	Gallbladder	18.1	Gallbladder	436	-96	(*43,44*)
FE-PE2I	Upper intestine		Bladder			(*45,46*)
Tetrafluoroborate	Stomach		Thyroid			(*47-49*)
			Thyroid			
PF-05270430	Gallbladder		GI Tract (males), Bladder (females)			(*50,51*)
	Gallbladder					
VAT	Liver		Gallbladder			(*52,53*)
FIMX	Bone		Bladder			(*54*); NIMH data
MNI-444	Gallbladder		Upper intestine			(*55,56*)
LMI1195	Bladder	100	Bladder	101.5	-1	(*57,58*)
MNI-659	Digestive tract		Gallbladder			(*31,59*)
HX4	Bladder	42	Bladder	27	56	(*60*)
FMeNER-D2	Kidney		Bladder			(*61,62*)
LSN3316612	Kidney		Bladder			(*63,64*)

[a] The organ doses of three tracers are not listed: ^{18}F-FPEB, ^{11}C-raclopride, and ^{11}C-UCB-J

The dose for ^{18}F-FPEB has been estimated twice in rhesus monkeys (*31,32*) and twice in humans (*29,30*). The target organ was identified as either the gallbladder (*31*) or the upper large intestine (*32*) in monkeys and as either the gallbladder (*30*) or the bladder (*29*) in humans.

For ^{11}C-raclopride, the gallbladder was identified as the target organ in monkeys by Herscovitch et al (*13*) and in humans by Slifstein et al (*12*). However, Ribeiro et al identified the kidneys as the target organ (*11*). Notably, the kidney dose of 40.6 μSv/MBq estimated by Ribeiro et al (*11*) is about one order of magnitude greater than the kidney dose estimated by Slifstein et al. at 6.8 μSv/MBq (*12*).

Since multiple studies are more likely to find at least one common target organ, these organ doses have not been included in the table.

Similarly, ^{11}C-UCB-J has two different target organs for males and females for both monkeys and humans. The only common organ is the liver, which is the target organ for male monkeys and women.

References

1. Sprague DR, Fujita M, Ryu YH, Liow JS, Pike VW, Innis RB. Whole-body biodistribution and radiation dosimetry in monkeys and humans of the phosphodiesterase 4 radioligand [(11)C](R)-rolipram: comparison of two-dimensional planar, bisected and quadrisected image analyses. *Nucl Med Biol.* 2008;35:493-500.

2. Lu JQ, Ichise M, Liow JS, Ghose S, Vines D, Innis RB. Biodistribution and radiation dosimetry of the serotonin transporter ligand 11C-DASB determined from human whole-body PET. *J Nucl Med.* 2004;45:1555-1559.

3. Tipre DN, Lu J-Q, Fujita M, Ichise M, Vines D, Innis RB. Radiation dosimetry estimates for the PET serotonin transporter probe [^{11}C]DASB determined from whole-body imaging in nonhuman primates. *Nucl Med Comm.* 2004;25:81-86.

4. Brown AK, Fujita M, Fujimura Y, et al. Radiation dosimetry and biodistribution in monkey and man of 11C-PBR28: a PET radioligand to image inflammation. *J Nucl Med.* 2007;48:2072-2079.

5. Hines CS, Liow J-S, Zanotti-Fregonara P, et al. Human biodistribution and dosimetry of 11C-CUMI-101, an agonist radioligand for serotonin-1A receptors in brain. *PloS one.* 2011;6:e25309.

6. Terry GE, Hirvonen J, Liow JS, et al. Biodistribution and dosimetry in humans of two inverse agonists to image cannabinoid CB1 receptors using positron emission tomography. *Eur J Nucl Med Mol Imaging.* 2010;37:1499-1506.

7. Liow JS, Kreisl W, Zoghbi SS, et al. P-glycoprotein function at the blood-brain barrier imaged using 11C-N-desmethyl-loperamide in monkeys. *J Nucl Med.* 2009;50:108-115.

8. Seneca N, Zoghbi SS, Liow JS, et al. Human brain imaging and radiation dosimetry of 11C-N-desmethyl-loperamide, a PET radiotracer to measure the function of P-glycoprotein. *J Nucl Med.* 2009;50:807-813.

9. Hirvonen J, Roivainen A, Virta J, Helin S, Nagren K, Rinne JO. Human biodistribution and radiation dosimetry of 11C-(R)-PK11195, the prototypic PET ligand to image inflammation. *Eur J Nucl Med Mol Imaging.* 2010;37:606-612.

10. Kumar A, Muzik O, Chugani D, Chakraborty P, Chugani HT. PET-derived biodistribution and dosimetry of the benzodiazepine receptor-binding radioligand (11)C-(R)-PK11195 in children and adults. *J Nucl Med.* 2010;51:139-144.

11. Ribeiro MJ, Ricard M, Bourgeois S, et al. Biodistribution and radiation dosimetry of [11C]raclopride in healthy volunteers. *Eur J Nucl Med Mol Imaging.* 2005;32:952-958.

12. Slifstein M, Hwang DR, Martinez D, et al. Biodistribution and radiation dosimetry of the dopamine D2 ligand 11C-raclopride determined from human whole-body PET. *J Nucl Med.* 2006;47:313-319.

13. Herscovitch P, Schmall B, Doudet DJ, Carson RE, Eckelman WC. Biodistribution and radiation dose estimates for [C-11]raclopride. *Journal of Nuclear Medicine.* 1997;38:951-951.

14. Bullich S, Slifstein M, Passchier J, et al. Biodistribution and radiation dosimetry of the glycine transporter-1 ligand 11C-GSK931145 determined from primate and human whole-body PET. *Mol Imaging Biol.* 2011;13:776-784.

15. Cropley VL, Fujita M, Musachio JL, et al. Whole-body biodistribution and estimation of radiation-absorbed doses of the dopamine D1 receptor radioligand 11C-NNC 112 in humans. *J Nucl Med.* 2006;47:100-104.

16. Moerlein S, Laforest R, Antenor J, Permutter J. Absorbed radiation dosimetry of the D1 ligand 11C-NNC 112 as determined by whole-body PET imaging of baboons. *Journal of Nuclear Medicine.* 2006;47:494P.

17. Petrulli JR, Hansen SB, Abourbeh G, et al. A multi species evaluation of the radiation dosimetry of [(11)C]erlotinib, the radiolabeled analog of a clinically utilized tyrosine kinase inhibitor. *Nucl Med Biol.* 2017;47:56-61.

18. Van Laere KJ, Sanabria-Bohorquez SM, Mozley DP, et al. (11)C-MK-8278 PET as a tool for pharmacodynamic brain occupancy of histamine 3 receptor inverse agonists. *J Nucl Med.* 2014;55:65-72.

19. Gallezot J-D, Beaver J, Nabulsi N, et al. [11C]PHNO studies in rhesus monkey: In vivo affinity for D2 and D3 receptors and dosimetry. *Journal of Nuclear Medicine.* 2009;50:601.

20. Mizrahi R, Rusjan P, Vitcu I, et al. Whole-body distribution and radiation dosimetry of 11C-(+)-PHNO, a D2/3 agonist ligand. *J Nucl Med.* 2012;53:1802-1806.

21. Parsey RV, Sokol LO, Belanger MJ, et al. Amyloid plaque imaging agent [C-11]-6-OH-BTA-1: biodistribution and radiation dosimetry in baboon. *Nucl Med Commun.* 2005;26:875-880.

22. O'Keefe GJ, Saunder TH, Ng S, et al. Radiation dosimetry of beta-amyloid tracers 11C-PiB and 18F-BAY94-9172. *J Nucl Med.* 2009;50:309-315.

23. Scheinin NM, Tolvanen TK, Wilson IA, Arponen EM, Nagren KA, Rinne JO. Biodistribution and radiation dosimetry of the amyloid imaging agent 11C-PIB in humans. *J Nucl Med.* 2007;48:128-133.

24. Lohith TG, Zoghbi SS, Morse CL, et al. Brain and whole-body imaging of nociceptin/orphanin FQ peptide receptor in humans using the PET ligand 11C-NOP-1A. *J Nucl Med.* 2012;53:385-392.

25. Kimura Y, Fujita M, Hong J, et al. Brain and whole-body imaging in rhesus monkeys of 11C-NOP-1A, a promising PET radioligand for nociceptin/orphanin FQ peptide receptors. *J Nucl Med.* 2011;52:1638-1645.

26. Bini J, Holden D, Fontaine K, et al. Human adult and adolescent biodistribution and dosimetry of the synaptic vesicle glycoprotein 2A radioligand 11C-UCB-J. *EJNMMI Research.* 2020;10:83.

27. Nabulsi NB, Mercier J, Holden D, et al. Synthesis and Preclinical Evaluation of 11C-UCB-J as a PET Tracer for Imaging the Synaptic Vesicle Glycoprotein 2A in the Brain. *J Nucl Med.* 2016;57:777-784.

28. Doss M, Kolb HC, Zhang JJ, et al. Biodistribution and radiation dosimetry of the integrin marker 18F-RGD-K5 determined from whole-body PET/CT in monkeys and humans. *J Nucl Med.* 2012;53:787-795.

29. Kessler RM, Seibyl J, Cowan RL, et al. Radiation Dosimetry of (18)F-FPEB in Humans. *J Nucl Med.* 2014;55:1119-1121.

30. Wong DF, Waterhouse R, Kuwabara H, et al. 18F-FPEB, a PET radiopharmaceutical for quantifying metabotropic glutamate 5 receptors: a first-in-human study of radiochemical safety, biokinetics, and radiation dosimetry. *J Nucl Med.* 2013;54:388-396.

31. Constantinescu C, Barret O, Tavares A, et al. A comparative study between whole-body dosimetry estimates of [18F]FPEB, [18F]MNI-659, and [18F]MNI-444 in non-human primates and humans. *Journal of Nuclear Medicine.* 2015;56:1016.

32. Bélanger MJ, Krause SM, Ryan C, et al. Biodistribution and radiation dosimetry of [18F]F-PEB in nonhuman primates. *Nucl Med Commun.* 2008;29:915-919.

33. Kimura Y, Simeon FG, Hatazawa J, et al. Biodistribution and radiation dosimetry of a positron emission tomographic ligand, 18F-SP203, to image metabotropic glutamate subtype 5 receptors in humans. *Eur J Nucl Med Mol Imaging.* 2010;37:1943-1949.

34. Maddahi J, Czernin J, Lazewatsky J, et al. Phase I, first-in-human study of BMS747158, a novel 18F-labeled tracer for myocardial perfusion PET: dosimetry, biodistribution, safety, and imaging characteristics after a single injection at rest. *J Nucl Med.* 2011;52:1490-1498.

35. Lazewatsky J, Azure M, Guaraldi M, et al. Dosimetry of BMS747158, a novel 18F labeled tracer for myocardial perfusion imaging, in nonhuman primates at rest. *Journal of Nuclear Medicine.* 2008;49:15P.

36. Fujimura Y, Kimura Y, Simeon FG, et al. Biodistribution and radiation dosimetry in humans of a new PET ligand, (18)F-PBR06, to image translocator protein (18 kDa). *J Nucl Med.* 2010;51:145-149.

37. Kurdziel KA, Kalen JD, Hirsch JI, et al. Human dosimetry and preliminary tumor distribution of 18F-fluoropaclitaxel in healthy volunteers and newly diagnosed breast cancer patients using PET/CT. *J Nucl Med.* 2011;52:1339-1345.

38. Kurdziel KA, Kiesewetter DO, Carson RE, Eckelman WC, Herscovitch P. Biodistribution, Radiation Dose Estimates, and In Vivo Pgp Modulation Studies of 18F-Paclitaxel in Nonhuman Primates. *Journal of Nuclear Medicine.* 2003;44:1330-1339.

39. Arakawa R, Takano A, Stenkrona P, et al. PET imaging of beta-secretase 1 in the human brain: radiation dosimetry, quantification, and test-retest examination of [18F]PF-06684511. *European Journal of Nuclear Medicine and Molecular Imaging.* 2020.

40. Takano A, Chen L, Nag S, et al. Quantitative Analysis of 18F-PF-06684511, a Novel PET Radioligand for Selective β-Secretase 1 Imaging, in Nonhuman Primate Brain. *Journal of Nuclear Medicine.* 2019;60:992-997.

41. Choi JY, Lyoo CH, Lee JH, et al. Human Radiation Dosimetry of [(18)F]AV-1451(T807) to Detect Tau Pathology. *Mol Imaging Biol.* 2016;18:479-482.

42. Huang YY, Chiu MJ, Yen RF, et al. An one-pot two-step automated synthesis of [18F]T807 injection, its biodistribution in mice and monkeys, and a preliminary study in humans. *PLoS One.* 2019;14:e0217384.

43. Doot RK, Dubroff JG, Scheuermann JS, et al. Validation of gallbladder absorbed radiation dose reduction simulation: human dosimetry of [(18)F]fluortriopride. *EJNMMI Phys.* 2018;5:21.

44. Laforest R, Karimi M, Moerlein SM, et al. Absorbed radiation dosimetry of the D3-specific PET radioligand [(18)F]FluorTriopride estimated using rodent and nonhuman primate. *Am J Nucl Med Mol Imaging.* 2016;6:301-309.

45. Lizana H, Johansson L, Axelsson J, et al. Whole-Body Biodistribution and Dosimetry of the Dopamine Transporter Radioligand (18)F-FE-PE2I in Human Subjects. *J Nucl Med.* 2018;59:1275-1280.

46. Varrone A, Gulyas B, Takano A, Stabin MG, Jonsson C, Halldin C. Simplified quantification and whole-body distribution of [18F]FE-PE2I in nonhuman primates: prediction for human studies. *Nucl Med Biol.* 2012;39:295-303.

47. Jiang H, Schmit NR, Koenen AR, et al. Safety, pharmacokinetics, metabolism and radiation dosimetry of (18)F-tetrafluoroborate ((18)F-TFB) in healthy human subjects. *EJNMMI Res.* 2017;7:90.

48. Marti-Climent JM, Collantes M, Jauregui-Osoro M, et al. Radiation dosimetry and biodistribution in non-human primates of the sodium/iodide PET ligand [(18)F]-tetrafluoroborate. *EJNMMI Res.* 2015;5:70.

49. O'Doherty J, Jauregui-Osoro M, Brothwood T, et al. (18)F-Tetrafluoroborate, a PET Probe for Imaging Sodium/Iodide Symporter Expression: Whole-Body Biodistribution, Safety, and Radiation Dosimetry in Thyroid Cancer Patients. *J Nucl Med.* 2017;58:1666-1671.

50. Constantinescu C, Cole P, Brown T, et al. Radiation dosimetry and biodistribution of [18F]PF-05270430, a radiotracer for phosphodiesterase 2A (PDE2A) in rhesus macaques and humans. *Journal of Nuclear Medicine.* 2018;59:1012.

51. Naganawa M, Waterhouse RN, Nabulsi N, et al. First-in-Human Assessment of the Novel PDE2A PET Radiotracer 18F-PF-05270430. *J Nucl Med.* 2016;57:1388-1395.

52. Karimi M, Tu Z, Yue X, et al. Radiation dosimetry of [(18)F]VAT in nonhuman primates. *EJNMMI Res.* 2015;5:73.

53. Laforest R, Lui H, HUssain J, Cummings K, Perlmutter J, Tu Z. Radiation Dosimetry on 18F-VAT in human. *Journal of Nuclear Medicine.* 2018;59:1002.

54. Zanotti-Fregonara P, Xu R, Zoghbi SS, et al. The PET Radioligand 18F-FIMX Images and Quantifies Metabotropic Glutamate Receptor 1 in Proportion to the Regional Density of Its Gene Transcript in Human Brain. *J Nucl Med.* 2016;57:242-247.

55. Barret O, Hannestad J, Alagille D, et al. Adenosine 2A Receptor Occupancy by Tozadenant and Preladenant in Rhesus Monkeys. *Journal of Nuclear Medicine.* 2014;55:1712-1718.

56. Barret O, Hannestad J, Vala C, et al. Characterization in humans of 18F-MNI-444, a PET radiotracer for brain adenosine 2A receptors. *J Nucl Med.* 2015;56:586-591.

57. Mistry M, Kagan M, Lazewatsky J, et al. Dosimetry in nonhuman primates of [18F]LMI1195, a novel PET tracer for imaging the cardiac sympathetic nervous system. *Journal of Nuclear Medicine.* 2010;51:1447.

58. Sinusas AJ, Lazewatsky J, Brunetti J, et al. Biodistribution and radiation dosimetry of LMI1195: first-in-human study of a novel 18F-labeled tracer for imaging myocardial innervation. *J Nucl Med.* 2014;55:1445-1451.

59. Barret O, Thomae D, Tavares A, et al. In vivo assessment and dosimetry of 2 novel PDE10A PET radiotracers in humans: 18F-MNI-659 and 18F-MNI-654. *J Nucl Med.* 2014;55:1297-1304.

60. Doss M, Zhang JJ, Belanger MJ, et al. Biodistribution and radiation dosimetry of the hypoxia marker 18F-HX4 in monkeys and humans determined by using whole-body PET/CT. *Nucl Med Commun.* 2010;31:1016-1024.

61. Seneca N, Andree B, Sjoholm N, et al. Whole-body biodistribution, radiation dosimetry estimates for the PET norepinephrine transporter probe (S,S)-[18F]FMeNER-D2 in non-human primates. *Nucl Med Commun.* 2005;26:695-700.

62. Takano A, Halldin C, Varrone A, et al. Biodistribution and radiation dosimetry of the norepinephrine transporter radioligand (S,S)-[18F]FMeNER-D2: a human whole-body PET study. *Eur J Nucl Med Mol Imaging.* 2008;35:630-636.

63. Lee JH, Liow JS, Paul S, et al. PET quantification of brain O-GlcNAcase with [(18)F]LSN3316612 in healthy human volunteers. *EJNMMI Res.* 2020;10:20.

64. Paul S, Haskali MB, Liow JS, et al. Evaluation of a PET Radioligand to Image O-GlcNAcase in Brain and Periphery of Rhesus Monkey and Knock-Out Mouse. *J Nucl Med.* 2019;60:129-134.